RECENT SYNTHETIC, STRUCTURAL, SPECTROSCOPIC, AND THEORETICAL STUDIES ON MOLECULAR PHOSPHORUS OXIDES AND OXIDE SULFIDES

J. CLADE, F. FRICK, AND M. JANSEN

Institut of Inorganic Chemistry, University of Bonn,
53121 Bonn, Germany

I. Introduction

The phosphorus oxides and oxide sulfides considered in this chapter have one topological feature in common: they all consist of four tetrahedral (PX_4) or Ψ-tetrahedral [EPX_3 (X = chalcogen, E = lone pair)] groups that are connected by three of their four vertices to form cage-like molecules. Phosphorus thus is surrounded by three bridging and one terminal chalcogen atoms, the latter position being occupied by a lone pair in the case of trivalent phosphorus. If all tetrahedral groups are identical, molecules of high symmetry (point group T_d) are generated, and the bridging chalcogen atoms are arranged as an ideal octahe-

dron that is interpenetrated by a regular tetrahedron of phosphorus atoms. This type of P_4X_6 skeleton frequently is referred to as adamantane like, $(CH)_4(CH_2)_6$.

On adding, removing, or substituting one or more of the terminally bound chalcogen atoms, the symmetry is lowered and the geometry of the P_4X_6 cage is distorted considerably. Because of the wide variety of possible modifications, this family of molecules is particularly well suited for comparative structural, spectroscopic, and theoretical studies aiming at a better understanding of the propagation of perturbations within molecules. This aspect will be emphasized throughout the chapter. As a typical example for the compounds under consideration, P_4O_8 is depicted in Fig. 1. The legend gives the nomenclature that will be used in order to describe subunits of the molecules.

Especially the phosphorus oxides are classics of inorganic chemistry and have gained considerable relevance for basic research and industrial chemistry as well. Single representatives of the title compounds have been mentioned already in the early times of quantitative chemistry, e.g., P_4O_{10} and P_4O_6 in 1816 (*1*). At the turn of the last century, some fundamental work on their synthesis and constitution had been

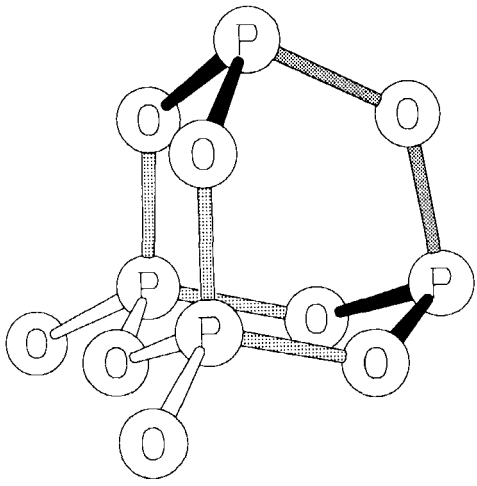

FIG. 1. Molecular structure of P_4O_8; schematic illustration of the different P—O linkages. (▨) P(III)—O_a; (■) P(III)—O_b; (▨) P(V)—O_b; and (□) P(V)—O_c. To specify the different atoms forming the phosphorus oxide molecules, the following nomenclature will be used: P(III) denotes a formally trivalent phosphorus atom; P(V), a formally pentavalent phosphorus atom. O_a denotes a bridging oxygen atom between two P(III) atoms; O_b, a bridging atom between a P(III) and a P(V) atom; and O_c, a bridging oxygen atom between two P(V) atoms. O_d denotes a terminally bonded oxygen atom.

TABLE I

KNOWN PHOSPHORUS OXIDES AND OXIDE SULFIDES, GENERALIZED FORMULA $P_4O_nS_m$

	$n + m$				
n	10	9	8	7	6
10	P_4O_{10}	—	—	—	—
9	X	P_4O_9	—	—	—
8	$P_4O_8S_2$	P_4O_8S	P_4O_8	—	—
7	$P_4O_7S_3$	$P_4O_7S_2$	P_4O_7S	P_4O_7	—
6	$P_4O_6S_4$	$P_4O_6S_3$	$P_4O_6S_2$	P_4O_6S	P_4O_6
5	$P_4O_5S_5$	X	X	X	X
4	$P_4O_4S_6$	X	X	X	X
3	$P_4O_3S_7$	$P_4O_3S_6$	X	X	X
2	$P_4O_2S_8$	X	X	X	X
1	P_4OS_9	X	X	X	X

accomplished (*2–5*). From that time to the mid-1960s, almost no activities took place in this field. Then, with increasing applications of X-ray crystallography to inorganic solids, the first reliable crystal structure determinations became available (*6, 7*). These results, addressed with structural and preparative issue, have been reviewed thoroughly by M. Meisel (*8*). Since then considerable progress has been made: The knowledge of the structures is far more complete, the synthetic approaches have been improved considerably, and extensive comparative spectroscopic investigations have been performed. These results deserve to be reviewed and discussed within a common context. The compounds that will be included are collected in Table I; the respective literature will be covered until the middle of 1993. Omitted are all investigations including matrix isolation techniques and the binary phosphorus sulfides.

II. Molecular Phosphorus Oxides

A. SYNTHESIS

1. General Remarks

The preferred route of preparing P_4O_6 and P_4O_{10} is the oxidation of elemental phosphorus with dry air, oxygen, N_2O, or mixtures of oxygen or N_2O with nitrogen (exceptions, see below). Although P_4O_6 and P_4O_{10}

are the anhydrides of phosphorous and phosphoric acids, respectively, it is impossible to prepare them by draining the corresponding acids even by treatment with strongly water-withdrawing agents. For the preparation of mixed phosphorus(III/V) oxides, at least two routes are reported in the literature; the first is based on the pyrolysis of P_4O_6 and the second, on the reduction of P_4O_{10} by elemental phosphorus. Some methods for the preparation of pure P_4O_7 have been published, but synthesis of pure phosphorus(III/V) oxides has continued to be a challenge in preparative chemistry and is a current subject of investigation.

2. *Phosphorus Pentoxide, or Phosphoric Oxide (P_4O_{10})*

a. Historical Aspects. In the last decade of the seventeenth century, R. Boyle (*9*) reported that the white fumes forming when phosphorus is burnt in air could be collected yielding a white, very hygroscopic powder. Analyses carried out by H. Davy (*10*), P. L. Dulong (*11*), and J. J. Berzelius (*1*) showed this substance to be an oxide of phosphorus, having the empirical composition "P_2O_5." Since then early investigators like J. J. Berzelius (*12*), Z. Delalande (*13*), R. F. Marchand (*14*), A. G. Grabowsky (*15*), T. Goldschmidt (*16*), and G. Pistor (*17*) have developed methods of preparing P_4O_{10} in a large scale.

b. Preparation from Elemental Phosphorus. Phosphorus pentoxide has usually been prepared—as was described by H. Davy already in 1821 (*10*)—by burning phosphorus in the presence of a sufficient quantity of dry air or oxygen. The crude product—which generally contains small amounts of lower phosphorus oxides—can be purified by sublimation in flowing dry oxygen (*18, 19*). The use of platinum asbetos as a catalyst in order to complete the oxidation, as recommended by R. Threlfall (*20*), is rather unsatisfactory, because asbestos adsorbs the pentoxide, thus removing the platinum from the reaction zone (*21*). On the technical scale, molten phosphorus is burnt in a stream of dry air in a specially designed burner made of stainless steel. The phosphoric oxide vapor is passed into a cooling chamber, where it condenses into a white powder (*22*). When produced under proper combustion conditions, the product contains only traces of lower oxides, but depending on the conditions of storage, small proportions of polyphosphoric acids may be present. Today, the commercially available phosphorus pentoxide contains 99,8% P_4O_{10}, less than 0,01% P_4O_6 and traces of As (<50 ppm), Fe (2 ppm), and other heavy metals, e.g., Pb (2 ppm) (*23*). In addition to the production of H_3PO_4 (for fertilizers), the following industrial uses of P_4O_{10} are worthy of note (*23*):

—Dehydration reactions (e.g., in methyl methacrylate manufacture);
—Manufacture of phosphoryl chloride and triethylphosphate;
—A vigorous drying agent; and
—An admixture for raising the softening point of asphalt.

c. Further Ways of Preparing Phosphorus Pentoxide. H. Davy (*24*) and J. Dalton (*25*) showed that white phosphorus reacts vigorously with SO_3, Cl_2O, ClO_2, and NO_2, forming P_4O_{10}. Other methods of preparing phosphorus pentoxide, e.g., the action of N_2O_3 on H_3PO_3 or PCl_3 (*26*), the reaction between $POCl_3$ and $KClO_3$ (*27*), or heating K_3PO_4, $K_4P_2O_7$, or Kurrol's salt with an excess of SO_3 (*28*), probably do not yield completely anhydrous phosphoric oxide.

3. Phosphorus Trioxide, or Phosphorous Oxide (P_4O_6)

a. Historical Aspects. Already in 1777, B. G. le Sage (*29*) succeeded in preparing phosphorous oxide by passing a slow stream of dry air over fragments of phosphorus. A. L. Lavoisier (*30*), and later P. A. Steinacher (*31*) and H. Davy (*10*) recognized that the oxide formed was somewhat different from that obtained by oxidizing phosphorus by combustion. Quantitative analyses carried out by P. L. Dulong (*11*) and J. J. Berzelius (*1*) showed the compositions of the oxides to be "P_2O_3" and "P_2O_5," respectively. Nevertheless, the existence of an "anhydride of phosphorous acid" remained doubtful (see, for example, Ref. *32*), until in 1886 T. E. Thorpe and A. E. Tutton (*2*) succeeded in preparing the oxide in a high degree of purity for the first time.

b. Preparation from Elemental Phosphorus. T. E. Thorpe and A. E. Tutton (*2*) burned phosphorus in one end of a long, horizontally placed combustion tube in a rapid stream of air drawn through the apparatus by a water pump. They condensed the resulting oxide by cooling the other end of the tube with iced water. It was not necessary to dry the air beforehand. Purification of the crude product was carried out by sublimination in a stream of dry CO_2 at 100°C, trapping the purified material in a cooled, U-shaped condenser adapted to the combustion tube. Further development in preparing P_4O_6 and purification of the crude material (which in most cases contains small amounts of dissolved phosphorus and higher phosphorus oxides) was achieved by Emeléus (*33*), who combusted phosphorus under reduced pressure, and C. C. Miller (*34, 35*). The latter pointed out that P_4O_6, if prepared by the method of Thorpe and Tutton (*2*), still contains unreacted phosphorus, which cannot be removed completely even by repeated distillation. However, recrystallization from CS_2 or light petroleum seemed to be successful. Final traces of dissolved phosphorus could be removed by

conversion into the red form via irradiating the crude material and subsequent distillation. If the latter procedure is repeated several times, the preceding treatment with solvents is not necessary. However, D. Heinz (*36*) has mentioned that even very pure P_4O_6 slowly decomposes when exposed to sunlight, forming phosphorus(III/V) oxides and elemental phosphorus.

The most recent development in the preparation methods of P_4O_6 on a laboratory scale is due to M. L. Walker in 1975 (*37*). He oxidized yellow phosphorus by air in the specially designed flow system described in Ref. *37*. On the industrial scale, several attempts have been made to develop a continuous process for producing P_4O_6 by combustion of phosphorus under special conditions. Large-scale availability of P_4O_6 is of considerable interest because it could replace PCl_3 as a precursor for the production of phosphorus(III) compounds on an industrial scale. In 1929, Wolf and Schmager (*38, 39*) were able to increase the yield of P_4O_6 up to 55% by using a mixture of O_2 and N_2 (3 : 1), using a pressure of 90–95 Torr and quenching the combustion products at ca. 50°C. In 1960, D. Heinz and E. Thilo applied for a patent (*36, 40, 41*) for the continuous production of P_4O_6 by oxidation of white phosphorus under reduced pressure.

At that time, they used a reaction temperature of 550–600°C, used a pressure of 70 Torr, and purified N_2O as the oxidizing agent. The yield of P_4O_6 with respect to P_4 was up to 70–80%. Further improvements of the production of P_4O_6 are listed in Table II (see also Ref. *42*, especially for thermodynamical and equilibrium considerations).

c. Further Ways of Preparing Phosphorus Trioxide. Many efforts have been made to prepare P_4O_6 from starting materials other than elemental phosphorus, e.g., H_3PO_3 or PCl_3. When A. Nacquet (*52*) mentioned that P_4O_6 is formed during the reaction of PCl_3 with H_3PO_3, many investigators tried to reproduce this finding. A. Gautier (*53*), A. Besson (*54, 55*), and L. J. Chalk and J. R. Partington (*56*) observed yellowish red, insoluble reaction products of varying compositions, the so-called "phosphorus suboxide." F. Krafft and R. Neumann (*57*) reported that they were successful in obtaining P_4O_6 from PCl_3 and H_3PO_3, but L. Wolf, E. Kalaehne and H. Schmager (*58*), as well as W. P. Jorissen and A. Tasman (*59*), failed to reproduce F. Krafft's results. In more recent papers, F. Hossenlopp *et al.* (*60*) have pointed out that the reaction between H_3PO_3 and PCl_3 leads to the formation of pyro- and probably polyphosphorous acids that decompose at higher temperatures, and D. Heinz (*36*) observed a solid red reaction product, from which—by thermal decomposition—P_4O_6 could be recovered at least in up to 0.5% yield.

TABLE II

DEVELOPMENT OF THE PROCEDURE FOR THE INDUSTRIAL PRODUCTION OF P_4O_6

Starting materials	Reaction temperature	Pressure	Special conditions	P_4O_6 yield	Ref.
$P_4/O_2/CO$, or $P_4/O_2/CO_2$	1800–2800°C, quenching at <500°C		Cooling, for example, with H_2O	H_3PO_3	*43*
Molten P, O_2/N_2 (1:1), N_2O, or NO_2/air (1:4)	620°C	70 T	KOH, Na_2CO_3, or $Ba(OH)_2$ as catalyst	80–95%	*44*
Gaseous P_4, O_2/N_2, or NO_2/air (1.5:1)	650°C	50 T	Unreacted P is recycled to the vaporizer	80 or 65%, respectively	*45*
P vapor, electrically excited CO_2	3000–12,000°C, quenching at <230°C		Irradiation (2–6 MHz)	36–46%	*46*
P vapor, electrically excited CO_2 or NO	0–100°C	0.001–0.1 atm	Irradiation (1000–5000 MHz)	24–28%	*47*
P vapor/CO_2 (1:1.5–1:15)	750–1500°C, quenching at <350°C		P_4O_6/P_4O_7 mixture	90–95%	*48*
P vapor/O_2/N_2 (1:ca.3:>0–4)	470°C		Quenching by addition of N_2	84%	*49*
P vapor/O_2/N_2 (1:ca.3:>0–25)	Quenching at 1500–2000°C, or at 1000–1600°C		Especially designed burner	>85%	*50, 51*
					43
P vapor/O_2/N_2	500–750°C, quenching at <350°C		Ading P_4O_6, removing solid products	>85%	

Other trials reported for the preparation of P_4O_6 from PCl_3 are

—Reaction between PCl_3 and formic acid (yielding H_3PO_3, CO, and HCl) (*61*);

—Action of acetic anhydride on PCl_3 (yielding acetyl chloride and a poorly characterized residue of varying composition) (*61, 62*);

—Action of PCl_3 on acetic acid, trichloroacetic acid, and butyric acid (no formation of P_4O_6 observed) (*59*);

—Action of PCl_3 on sodium formate (yielding NaCl, H_3PO_3, and CO) (*59*);

—Reaction between PCl_3 and $(Et_3Sn)_2O$ (*63*); and

—Reaction between PCl_3 and $(N(CH_3)_4)_2SO_3$ in liquid SO_2 (yielding up to 80% P_4O_6) (*36, 64*).

4. Phosphorus(III/V) Oxides

a. Historical Aspects. In 1884, P. Hautefeuille and A. Perrey (*65*) combusted phosphorus under conditions that may have led to the formation of phosphorus(III/V) oxides, but they believed to have obtained a crystalline variant of P_4O_{10}. Two years later, T. E. Thorpe and A. E. Tutton (*2*) showed that a distinct crystalline oxide of the empirical composition "PO_2" could be obtained by heating the mixed products from the slow combustion of phosphorus in an evacuated sealed tube at 290°C.[1] Building on the results obtained by Thorpe and Tutton, C. A. West (*5*) prepared the oxide by thermal decomposition of P_4O_6 at 200–250°C for two to three days in an atmosphere of dry carbon dioxide. The crude material was purified subsequently by repeated sublimation. Due to its low solubility in most organic solvents and its tendency to polymerize or to decompose at higher temperatures, molecular weight determinations attempted by the early investigators failed (see, for example, Ref. *5*). Corresponding to dinitrogen tetroxide, N_2O_4, the substance was called "phosphorus tetroxide" or "phosphorosophosphoric oxide," and the formula "P_2O_4" was assigned to it. The formation of "phosphorus tetroxide" was observed subsequently by a number of researchers: by C. C. Miller (*67*), as a product of the oxidation of P_4O_6 in presence of water vapor, by E. Britzke and N. Pestow (*68*), as well as P. H. Emmett and J. F. Schulz (*69*), as a product of the reaction between phosphorus vapor and CO_2, and by S. Brunauer and J. F. Schultz (*70*), as a product of the reaction between phosphorus and water vapor at 1000–1200°C. Nevertheless, the true nature of "P_2O_4" remained unclear until 1964, when D. Heinz *et al.* (*71, 72*) discovered that these samples represent in fact a mixture of two different solid solutions. The orthorhombic α-phase has been reported to have the empirical composition $P_4O_{8.1-9.2}$ and to consist of P_4O_8, P_4O_9, and occasionally P_4O_{10} molecules, whereas the monoclinic β-phase has been reported to have the composition $P_4O_{7.7-8.0}$ and to contain P_4O_7 and P_4O_8 molecules in a solid solution.

b. Preparation of Phosphorus(III/V) Oxides. It was assumed that phosphorus(III/V) oxides could not be synthesized as pure solids, forming solid solutions as a rule. Such phases usually were prepared by thermal decomposition of P_4O_6 (*2, 5*). Another method, based on the reduction of P_4O_{10} by red phosphorus at 450–525°C, has been reported by D. Heinz *et al.* (*71, 72*). They pointed out that—in both cases—higher

[1] Under somewhat similar conditions, E. J. Russell (*66*) was able to recover the same substance.

reaction temperatures lead to the formation of oxygen-rich products and vice versa. The reduction of phosphorus(III/V) oxide mixtures with red phosphorus yields oxide mixtures with a lower oxygen content.

A few years later, D. Heinz *et al.* (*73*) discovered that phosphorus(III/V) oxides (β-phase) are also formed by the oxidation of P_4O_6 in carbon tetrachloride with oxygen. By this reaction, P_4O_7/P_4O_8 mixtures with an overall composition $P_4O_{7.0-7.9}$ are obtained. Occasionally phosphorus(III/V) oxide mixtures are by-products of a process for the production of P_4O_6 on a technical scale (*48, 74*). Although M. Loeper and U. Schülke (*75*) have mentioned that P_4O_7 sublimes at 50–80°C (100–200 Pa) and P_4O_8 at 150–160°C from phosphorus(III/V) oxide mixtures, it seemed to be impossible to separate the three oxides from each other even by repeated sublimation. For gas phase equilibria between phosphorus(III/V) oxides, see Ref. *42*.

c. Preparation of Pure Phosphorus(III/V) Oxides. M. L. Walker and J. L. Mills prepared P_4O_7 by heating a solution of P_4O_6 in dry diglyme at 135–140°C (*37*), by heating a solution of P_4O_6 in Benzene in presence of traces of moisture, or by stirring a solution containing equimolar quantities of P_4O_6 and triphenyl phosphine oxide in dry tetrahydrofurane at room temperature (*76, 77*). The observation that the substance partly decomposed upon sublimation indicates that it probably still contained traces of the solvent.

A better method for preparing pure P_4O_7 was discovered by M. Jansen and M. Moebs (*79*).[2] They oxidized P_4O_6 in a closed system and an oxygen-buffered atmosphere. The reaction vessel consisted of a V-shaped glass tube, one end containing P_4O_6 and the other containing dry silver oxide. The tube was sealed under argon, and the end that contained the silver oxide was placed into a furnace and heated at 190–210°C. Under these conditions, the oxygen pressure above Ag_2O is sufficient to oxidize the P_4O_6 that is present in the gas phase. According to Gibb's rule, P_4O_7 is the only phosphorus oxide that can coexist under equilibrium conditions with an excess of unchanged P_4O_6 as a condensed phase. By this reaction, P_4O_7 is formed as colorless, transparent, highly lustrous crystals just above the part of the tube that is heated. Further investigations about the synthesis of P_4O_7 by oxidizing P_4O_6 with highly diluted oxygen (obtained from a special designed argon/oxygen mixing apparatus) is still in progress (*80, 81*). Pure P_4O_7 is also obtained in up to 20% yield by the oxidation of P_4O_6 with

[2] Pure P_4O_7 is also formed in the reaction of P_4O_6 with alkali metal oxides, e.g., K_2O or Cs_2O (*78*).

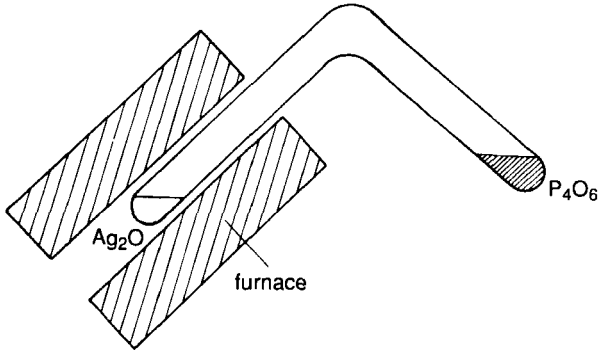

FIG. 2. Apparatus for the preparation of pure P_4O_7 (*79*).

$(CH_3)_3N{\cdot}SO_3$ (1,2-dichloroethane, Soxhlet apparatus) or with 1,4-benzodioxane·SO_3 (THF). Oxidation of P_4O_6 with 1,4-dioxane·SO_3 yields mixtures of P_4O_7 and P_4O_8 (*82*).

Although crystals of the β-phase of phosphorus(III/V) oxides with a high content of P_4O_8 can be obtained (*7, 71, 72, 73*),[3] nobody has yet been able to isolate the pure oxide. D. Heinz *et al.* assumed that phosphorus(III/V) oxide mixtures that contain >95% of P_4O_8 form only amorphous solids. This may be due to the fact that P_4O_8 has the lowest molecular symmetry of all phosphorus oxides considered here. Further investigation of this subject is still in progress.

M. Jansen and B. Lüer have been successful in isolating pure P_4O_9 from phosphorus(III/V) oxide mixtures by dissolving P_4O_7 and P_4O_8 with 1,4-dioxane and subliming the residue, which consisted mainly of the less soluble P_4O_9 (*83*). Recent experiments (*80*) indicate that crude P_4O_9 is also accessible by the reaction of P_4O_{10} with red or white phosphorus at 450°C and subsequent sublimation from 390°C to room temperature.[4] X-ray-powder diffraction and ^{31}P MAS–NMR data prove that the amount of P_4O_8 in the product obtained is less than 3%.

[3] By oxidizing P_4O_6 with tetrabutylammoniumperiodate in dry CH_2Cl_2, occasionally a solution that contains P_4O_8 as the only phosphorus oxide was obtained, as indicated by ^{31}P NMR spectroscopy. Nevertheless, attempts to isolate the substance have failed, because the product polymerizes when the solvent is drawn off (*80*).

[4] The so-called "phosphorus suboxide" (see, for example, Ref. *84*) reduces P_4O_{10} already at lower temperatures, e.g., 350°C, forming phosphorus(III/V) oxide mixtures with a high content of P_4O_9 (*85*).

B. Crystal and Molecular Structures

1. *Historical Aspects*

By the end of the nineteenth century, molecular weight determinations carried out by means of vapor density measurements proved that phosphorus(V) and phosphorus(III) oxide in the gaseous state consist of molecules of the compositions P_4O_6 (*3, 86*) and P_4O_{10} (*87*), respectively. However, their molecular structures remained uncertain (see, for example, Ref. *88*) until adequate techniques for structure determination such as electron and X-ray diffraction became available (*6, 7, 72*).

2. *Determination of the Molecular Structures of Phosphorus Oxides in the Gaseous State*

The structures of P_4O_6 and P_4O_{10} were first investigated by means of electron diffraction. L. R. Maxwell, S. B. Hendricks, and L. S. Deming (*89*) reported the structure of P_4O_6, but were unable to deduce the molecular structure for P_4O_{10}. The authors erroneously attributed a lower symmetry than T_d. The correct structure of P_4O_{10} was found by G. C. Hampson and A. J. Stosick (*90*). Several investigations followed with the goal of improving the accuracy of the bond lengths and angles (see Tables III and IV).

Concerning the phosphorus(III/V) oxides, no structural data in the gaseous state are available; the only attempt (*89*) to determine the molecular structure of one of the phosphorus(III/V) oxides, P_4O_8, has failed.

3. *Determination of the Molecular Structures in the Solid State*

a. Crystal Structure of P_4O_{10}. Phosphorus(V) oxide was the first oxide of phosphorus that has been structurally characterized by means of X-ray crystallography. There are three crystalline modifications (*95–97*), which can be designated as M, R, and S modifications, accord-

TABLE III

Molecular Structure of P_4O_6 in the Gaseous State

	Ref. *89*	Ref. *90*	Ref. *91*
P—O	1.67(3) Å	1.65(2) Å	1.638(3) Å
O—P—O		99(1)°	99.8(0.8)°
P—O—P	128.5(1.5)°	127.5(1.0)°	126.4(0.7)°

Note. Standard deviations are given in parentheses.

TABLE IV

MOLECULAR STRUCTURE OF P_4O_{10} IN THE GASEOUS STATE

	Ref. *90*	Ref. *92*	Ref. *93*
$P—O_{br}$	1.62(2) Å	1.60(1) Å	1.604(3) Å
$P—O_t$	1.39(2) Å	1.40(3) Å	1.429(4) Å
$O_{br}—P—O_{br}$	101.5(1.0)°		101.6(8)°
$O_{br}—P—O_t$	116.5(1.0)°		116.5(3)°
$P—O_{br}—P$	123.5(1.0)°	124.3(1.0)°	123.5(7)°

Note. Standard deviations are given in parentheses.

ing to a suggestion of E. Thilo and E. Wieker (*94*). In this chapter, only the structure of the metastable modification, which consists of P_4O_{10} molecules (M modification), will be considered, because the other modifications consist of polymeric networks of tetrahedral PO_4 units connected via common vertices. The M modification is the commercially available form of phosphorus(V) oxide. Its crystal structure was refined by C. D. J. Cruickshank (*98*) using the experimental data collected by H. C. J. de Decker and C. H. McGillavry (*95*) (see Table V). Surprisingly this refinement yielded different values for the bond lengths of the two crystallographically independent $P(V)–O_d$ bonds. These values, 1.41(2) and 1.51(4) Å, respectively, should be equivalent within the T_d symmetry of the free molecule. Because they differ by an unreasonably large amount, a redetermination of the crystal structure of P_4O_{10} was undertaken (*99*). The geometry of P_4O_{10} as obtained by this latter refinement is consistent with the point group T_d and is also in good agreement with the electron diffraction results for the gaseous oxide.

TABLE V

MOLECULAR STRUCTURE OF P_4O_{10} IN THE SOLID STATE

	Ref. *95*	Ref. *98*	Ref. *99*
$P(V)—O_c$	1.63 Å	1.58(2) Å	1.599(3) Å
$P(V)—O_d$	1.41 Å	1.41(2) and 1.51(4) Å, respectively	1.441(4) Å
$O_c—P(V)—O_c$	102.3°	101.0°	102.2(2)°
$O_c—P(V)—O_d$	115.6°	117.0°	116.1(2)°
$P(V)—O_c—P(V)$	121.4°	124.3°	122.8(1)°

Note. Standard deviations are given in parentheses.

b. Crystal Structure of P_4O_6. Phosphorus(III) oxide was the last oxide of phosphorus to be characterized structurally in the solid state (*100, 101*). This is due to its low melting point, which introduces difficulties for the growth of single crystals. These have been met successfully by growing crystals from the melt in Lindemann glass capillaries *in situ* on a diffractometer. In the course of low-temperature X-ray investigations (*101*), Guinier photographs indicated a structural phase transition of higher order taking place at -45 ± 4°C. The determination of the structure of the low-temperature modification (*102*) revealed that the molecular geometry of P_4O_6 does not change at the phase transition, instead the molecular packing is changing slightly (see below).

The bond distances in solid P_4O_6 [1.653(3) Å] are larger than those determined for gaseous P_4O_6 [1.638(3) Å]. However, the confidence ranges for the bond length distributions still overlap.

c. Crystal Structure of P_4O_9. The crystal structure of P_4O_9 was first investigated in 1964 (*6*). This determination was affected by using a mixed crystal of the empirical composition $P_4O_{8.96}$. Based on the experimental data obtained, a refinement (*93*) was carried out. A more precise determination (lower standard deviations) for pure P_4O_9 (*83*) has been supplied. The bond lengths and angles obtained in these three investigations are listed in Table VI.

d. Crystal Structure of P_4O_8. The only structural data on the crystal structure of P_4O_8 were obtained again from a mixed crystal with the empirical composition $P_4O_{7.9}$ (*7*). This indicates that some of the P_4O_8 molecules are substituted by P_4O_7 molecules, and thus the data obtained are less reliable. A similar caveat holds for the results of a structure refinement (*91*) based on the same diffraction data.

TABLE VI

BOND LENGTHS (Å) IN SOLID P_4O_9

	Ref. *6*	Ref. *93*	Ref. *83*
P(III)—O_b	1.66(1)	1.661(13)	1.675(2)
P(V)—O_b	1.60(1)	1.605(17)	1.573(3)
P(V)—O_a	1.59(1)	1.590(12)	1.608(2)
P(V)—O_d	1.44(2)	1.418(14)	1.443(2)

Note. Standard deviations are given in parentheses.

TABLE VII

BOND LENGTHS (Å) IN PHOSPHORUS OXIDES

	P_4O_6 (*100*)	P_4O_7 (*78*)	P_4O_8 (*91*)	P_4O_9 (*83*)	P_4O_{10} (*99*)
P(III)—O_a	1.653(3)	1.640(9)	1.633(10)		
P(III)—O_b		1.680(6)	1.672(14)	1.675(2)	
P(V)—O_b		1.590(8)	1.576(17)	1.573(3)	
P(V)—O_c			1.596(9)	1.608(2)	1.599(3)
P(V)—O_d		1.450(5)	1.414(15)	1.443(2)	1.441(4)

Note. Standard deviations are given in parentheses.

e. Crystal Structure of P_4O_7. The structure of P_4O_7 was determined in 1981 independently by K.-H. Jost and M. Schneider (*103*) and by M. Jansen and M. Moebs (*78, 79*), the results being virtually identical.

f. Comparison of the Molecular Structures of the Phosphorus Oxides. Figures 1 and 3–6 illustrate the structures of the molecules P_4O_n (n = 6–10) with a schematic presentation of the different P–O linkages; Table VII provides a comparison of corresponding bond lengths, employing the most accurate data available. Here, distortion of the P_4O_6 cage due to the addition of terminally bonded oxygen atoms is illustrated. Whereas the P_4O_6 molecule has only one type P–O linkage, there are three different types in the P_4O_7 and P_4O_9 molecules and even four in P_4O_8. These show considerable variations in their lengths. The distortion of the molecules is reflected most clearly by the P–O_b distances.

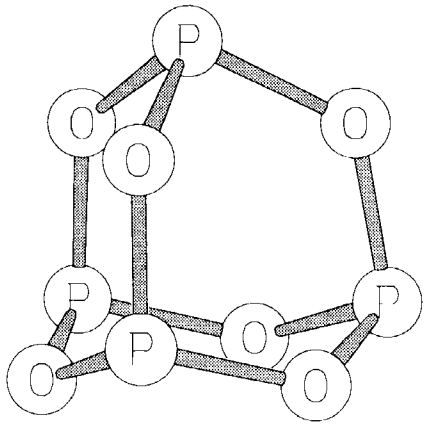

FIG. 3. Molecular structure of P_4O_6. See legend for Fig. 1.

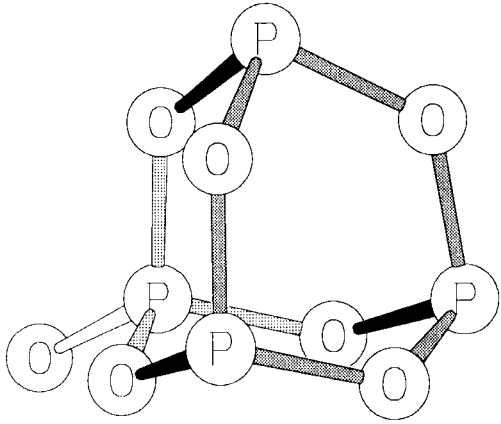

FIG. 4. Molecular structure of P_4O_7. See legend for Fig. 1.

P(III)–O_b, e.g., in P_4O_9 (1.680 Å), is 6.5% longer than the P(V)–O_b linkage (1.573 Å). Generally, the bonds starting from formal pentavalent phosphorus atoms are shorter than those starting from trivalent phosphorus atoms. In addition, a propagation of the distortion introduced by the terminal oxygen atoms throughout the bonds of the P_4O_6 cage can be identified. By comparing analogous linkages in the different phosphorus oxide molecules, it can be seen that in general the P_4O_6 cage is contracted upon successive oxidation of the phosphorus atoms

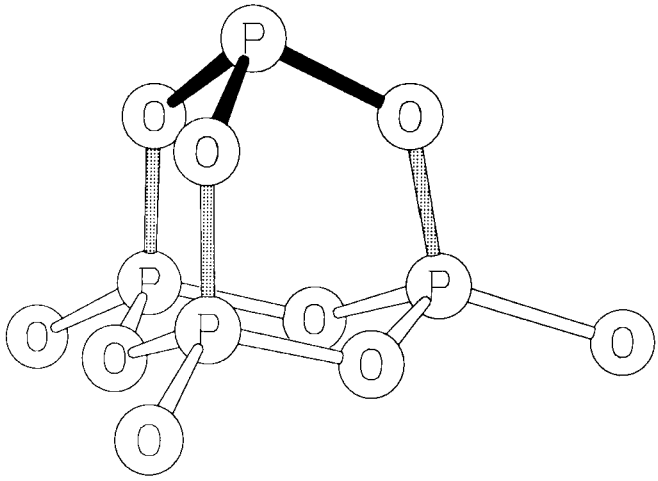

FIG. 5. Molecular structure of P_4O_9. See legend for Fig. 1.

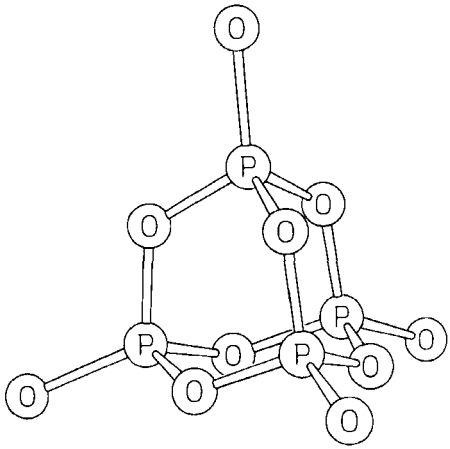

FIG. 6. *Molecular structure of* P_4O_{10}. See legend for Fig. 1.

(see also Section III.B). Table VIII gives the bond angles in the phosphorus oxide molecules. As a rule, the angles involving P(III) atoms are always smaller than those involving P(V) atoms because the lone pair of P(III) requires more space than a P(V)–O_d linkage (*104*). Analogous bond angles in the different phosphorus oxide molecules expand when terminally bonded oxygen atoms are added.

Although most of the phosphorus atoms in the oxides are crystallographically independent, the symmetries of the molecules as determined for the crystalline state do not differ significantly from those

TABLE VIII

BOND ANGLES (°) IN PHOSPHORUS OXIDES (*78, 83, 91, 99, 101*)

	P_4O_6	P_4O_7	P_4O_8	P_4O_9	P_4O_{10}
O_a—P(III)—O_a	99.6	100.0			
O_a—P(III)—O_b		98.3	98.5		
O_b—P(III)—O_b		97.4	97.3		
O_b—P(V)—O_b		103.5	105.0		
O_b—P(V)—O_c			102.7	103.2	
O_c—P(V)—O_c				100.8	102.2
O_b—P(V)—O_d		114.9	115.6	118.7	
O_c—P(V)—O_d			113.6	114.4	116.1
P(III)—O_a—P(III)	127.0	128.1	130.1		
P(III)—O_b—P(V)		123.9	124.4	126.3	
P(V)—O_c—P(V)			121.2	122.4	122.8

found or expected for the gaseous state and are expressed by the same point groups (*78, 79, 82, 83, 99, 101*).

g. Molecular Packing of the Phosphorus Oxides in the Solid State. The phosphorus oxides P_4O_7, P_4O_8, P_4O_9, and P_4O_{10} show close relations in the metrices and symmetries of their space groups (*105*). K.-H. Jost realized that the lattice constants of P_4O_8 resemble those of a monoclinic unit cell of rhombohedral P_4O_9 (only the c axis is half as long). P_4O_7 has nearly the same unit cell parameters as P_4O_8 (*83*). Eventually, it was demonstrated that a monoclinic setting with close relationship to the crystal lattices of the other phosphorus oxides can be found for rhombohedral P_4O_{10} too (Fig. 7) (*105*).

The unit cells of all these oxides can be reduced to one common, approximately body-centered "pseudo-unit cell" with $a \approx b \approx c$ and

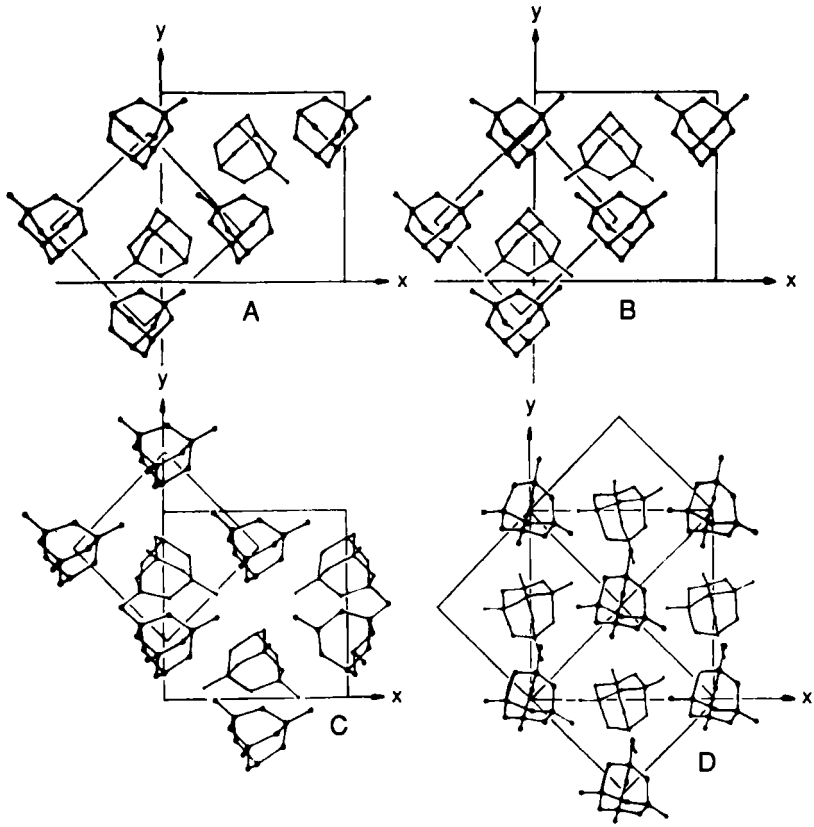

FIG. 7. Projection of the crystal structures of P_4O_7 (A), P_4O_8 (B), P_4O_9 (C), and P_4O_{10} (D) along the c axis of the monoclinic (A, B) and pseudomonoclinic (C, D) settings (*105*).

$\alpha \approx \beta \approx \gamma \approx 90°$ containing two molecules. This body-centered packing of molecules is realized with highest possible structural symmetry (point group, T_d; space group, $I\bar{4}3m$) for hexamethylenetetramine. By means of a systematic reduction of the space group symmetry, this structure can be correlated with those of the different phosphorus oxides. The relationships among the phosphorus oxides have been displayed in Fig. 8 using a tree-like structure to exhibit the hierarchic order of group–subgroup relationships (see also Ref. *105*).

The observed intermolecular distances show that there are only van der Waals-type intermolecular forces. Obviously, the structural relations of the phosphorus oxides are due to the endeavor to adopt an optimally dense packing (see also Section III.B). Here the rules formulated by A. I. Kitaigorodski (*106*), i.e., maximal space-filling structures

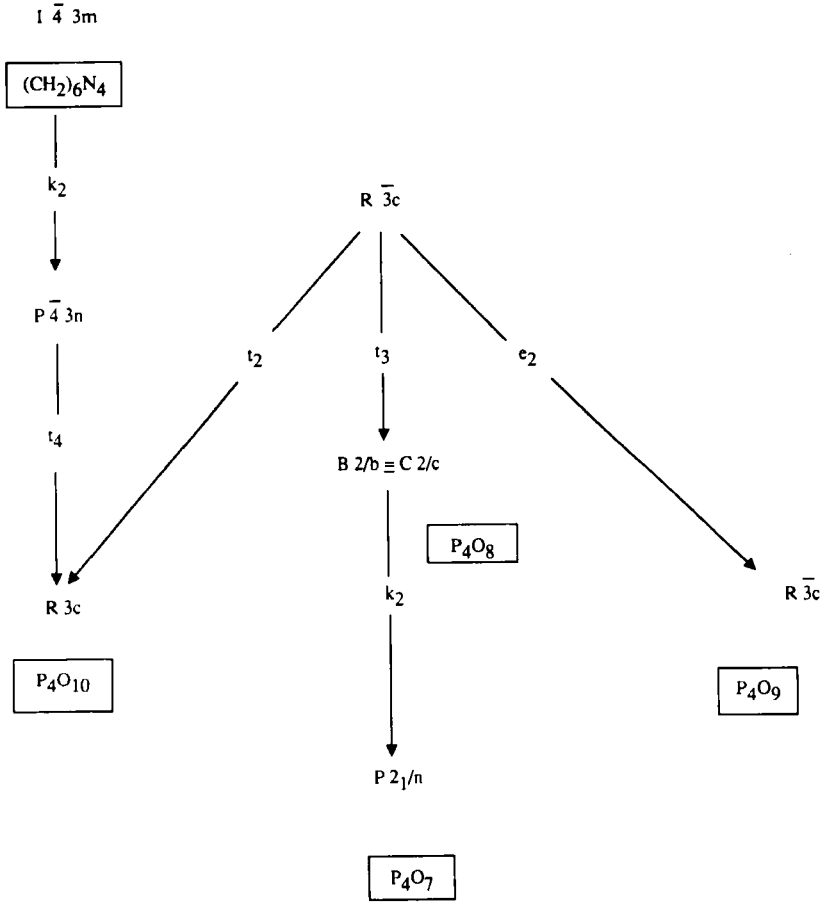

FIG. 8. Group–subgroup relationships among phosphorus oxides (*105*).

are created by the matching of concave and convex regions at the surfaces of neighboring molecules, are fulfilled. As a consequence, packings of molecules frequently resemble those of metals or alloys. In case of the phosphorus oxides, the tungsten type of arrangement is adopted.

It has been determined that (surprisingly!) P_4O_6 adopts neither this packing (*101, 102*) nor an fcc arrangement such as As_4O_6. The structures of both modifications are formed of "rods" of P_4O_6 molecules aligned along one of their threefold symmetry axes. The rods are parallel to the crystallographic *a* axis and are closely packed in the *bc* plane. The P_4O_6 molecules of the monoclinic high-temperature modification show a crystallographic mirror plane that is lost upon the transition to the triclinic low-temperature modification (*102*). The mirror plane defined by two phosphorus and two oxygen atoms is retained during phase transition, but loses its special orientation with respect to the crystal lattice, thus lowering the crystal symmetry to triclinic. Table IX gives a summarizing overview of the crystal structures of all five molecular phosphorus oxides.

TABLE IX

CRYSTALLOGRAPHIC DATA OF MOLECULAR PHOSPHORUS OXIDES

Oxide	Crystallographic symmetry	Space group	Lattice constant[a]
P_4O_6 (HT)	Monoclinic	$P2_1/m$	a = 6.422(1) Å b = 7.877(2) Å c = 6.786(3) Å β = 106.1(1)°
P_4O_6 (LT)	Triclinic	$P\bar{1}$	a = 6.39(1) Å b = 7.86(1) c = 6.77(1) Å α = 87.7(2)° β = 107.1(2)° γ = 91.5(1)°
P_4O_7	Monoclinic	$P2_1/n$	a = 9.807(2) Å b = 9.973(4) Å c = 6.840(2) Å β = 96.83(1)°
"P_4O_8" ($P_4O_{7.9}$)	Monoclinic	$C2/c$	a = 9.66(4) Å b = 10.10(4) Å c = 6.93(3) Å β = 96.8(3)°
P_4O_9	Trigonal–rhombohedral	$R\bar{3}c$	a = 10.0057(2) Å α = 57.947(2)°
P_4O_{10}	Hexagonal	$R3c$	a = 10.3035(9) Å c = 13.5102(19) Å

[a] Standard deviations are given in parentheses.

TABLE X

VIBRATIONAL SPECTRA OF P_4O_6 (*114*)

IR (CS_2 solution)	Raman	Assignment
285 vw	285 vw	E
302 vw	302 (10)	F_2
370 w	370 (variable)	Dissolved P_4?
407 vs	407 (18)	F_2
	465 (variable)	Dissolved P_4
549[a] w		
569[a] w	569 (3,p)	A_1
587[a] w		302 + 302/825 = 604/587
	613 (100,p)	A_1
643 vs	643 (55)	F_2
687[a] w	691 (1)	E
702[a] w		302 + 407 = 709
718 vw		?
808 vw		407 + 407 = 814
832[a] m		F_1
849[a] w		569 + 285 = 854
919 vvs	919 (5)	F_2
1018 m		407 + 613 = 1020
1048 w		407 + 643 = 1050
1180 w		919 + 302 = 1221?
1258 s		613 + 643 = 1256
1273 s		643 + 643 = 1286
1313 w		919 + 407 = 1326
1460 vw		832 + 643 = 1475
1545 w		919 + 643 = 1562
1625 w		832 + 832 = 1664?
1880 vw		919 + 919 = 1832??

[a] Very weak or (probably) absent in the vapor spectrum.

C. SPECTROSCOPY

1. Vibrational Spectroscopy

a. P_4O_6 and P_4O_{10}. The fundamental work carried out by H. Gerding. H. v. Brederode, and H. C. J. de Decker [Raman spectra and calculation of force constants (*107–110*)] has been completed by T. A. Sidorov and N. N. Sobolev [IR spectra (*111, 112*)], by D. H. Zijp (*113*), and by A. C. Chapman (*114*) (vibrational assignment and calculation of improved force constants). The frequencies and intensities of the bands observed, and the assignment (as given by Chapman) are listed in Tables X and XI.[5] Force constants for the P_4O_6 and P_4O_{10} molecules

[5] The gas phase vibrational spectra of P_4O_6 and P_4O_{10} are reported in Refs. *115* and *116*; for matrix IR spectra, see Refs. *117–119*.

TABLE XI

VIBRATIONAL SPECTRA OF P_4O_{10} (*114*)

IR	Raman	Assignment
	194 vw?	
	237 vw?	
	257 s	E
270 } s	278 m	F_2
280 }		
330 w; sh		
	355 vw br?	
414 } s	424 s	F_2
421 }		
510?m; br		
	559 s	A_1
573 s	576 vw	F_2
610 vw; sh		
670 w; sh		
698 w; sh	710 vw?	
	720 s	A_1
760 vs; m	760 vw	F_2
820 } v;sh		
838 } m	828 vw	F_1, E?
846 }		?
1010 vs		F_2
1110 m		$556 \cdot 2 = 1112$
1130 m		$556 + 573 = 1129$
1181 w		$760 + 424 = 1184$
1242 w		?
1273 m; w		$720 + 556 = 1276$
1390 vs	1385 m	F_2
	1418 s	A_1
1628 m; s		$820 \cdot 2 = 1640$
1695 m; s		$846 \cdot 2 = 1692$
1720 w		$1010 + 720 = 1730$
1770 w		$1010 + 760 = 1770$
1835 vw		$1413 + 424 = 1837$
1880 vw		?
1935 vw		$1390 + 559 = 1949$
2000 vw		$1010 \cdot 2 = 2020$
2060 vvw		$1384 + 720 = 2094$?
2150 vw		$1413 + 760 = 2173$

were first calculated by H. v. Brederode and H. Gerding (*109*) using Bjerrum's simple valence force field system. Table XII gives a list of the improved force constants (obtained by using the extended force field method) given by Zijp (*113*).

TABLE XII

FORCE CONSTANTS (mdyn/Å) CALCULATED FOR P_4O_6 AND P_4O_{10}

	P_4O_6		P_4O_{10}	
	I	II	I	II
$f(PO_{br})$	4.787	3.825	5.25	3.902
$f(PO_t)$			11.0	10.84
$d(PO_{br}P)$	0.51	0.38	0.35	0.42
$d(O_{br}PO_{br})$	0.153	0.125	0.35	0.21
$d(O_{br}PO_t)$			0.61	0.557
F_q[a]		0.11		0.11
F_s		0.44		0.69
F_t				0.08

Note. I, simple force field; II, extended force field (*113*). A determination carried out by Chapman (*114*) using a modified Urey–Bradley force field yielded similar results. In the case of P_4O_{10}, a slight improvement of the force field has been achieved by Muldagaliev and coworkers (*120*).

[a] F_q, F_s, and F_t are the coefficients for the second-order development of the potential energy, having the form

$$2V' = F_q \sum^{12} r^2_{O_{br}O_{br}} + F_s \sum^{6} r^2_{PP} + F_t \sum^{12} r^2_{PO_t}.$$

For these calculations, the bond lengths and angles from electron diffraction data (*89, 90, 93*; see also Section II.B) have been used. Considering the empirical correlation between the valence stretching constants and the bond order [according to D. W. J. Cruickshank (*123*)[6]], a bond order of 1.0625 was derived for P–O in P_4O_6 (*114*), already suggesting a slight *d*-orbital participation. For P_4O_{10}, the bond orders are 1.33 ($P–O_{br}$) and 2.2 ($P–O_t$) (*114*), respectively. This has been taken as support for the assumption that *d*-orbital participation in the $P–O_{br}$ bonds is much stronger for P_4O_{10} than that for P_4O_6.

Although very accurate structural data for the P_4O_7 and P_4O_9 molecules are available (see Section II.B), no force constants have been reported so far. For the purpose of discussing the relation between molecular geometries and chemical bonding (which is an important topic of this chapter), such calculations would be very desirable.

[6] A comprehensive discussion about vibrational spectra and force constants of phosphorus compounds is supplied in Ref. *124*.

TABLE XIII

VIBRATIONAL FREQUENCIES OF PHOSPHORUS (III/V) OXIDES IN SOLID ARGON (*117*)

P_4O_7	P_4O_8	P_4O_9	Assignment
1379.4	1401.6	1406.4	P=O stretch; A_1
	1384.7	1397.8	P=O stretch; B_2 or E, respectively
984.8	1004.3	1019.4	P_4O_6 cage modes
976.3	995.9	1011.9	
966.4		1005.7	
653.5	683.7	706	P_4O_6 cage modes
649.6	669.3		
634.6			
625.9	614.5		P_4O_6 cage modes, A_1
537.5	556	563.4	P=O bending
427.6	440.4	431	P_4O_6 cage modes
391.0			

b. Phosphorus(III/V) Oxides. In 1989, Z. Mielke and L. Andrews (*117*) recorded matrix-infrared spectra of phosphorus oxides that had been produced by oxidizing P_4O_6 with O_3. For P_4O_6 and P_4O_{10}, the results agreed with earlier data [see Chapman (*114*)]. Table XIII gives a list of the frequencies observed for the phosphorus(III/V) oxides and their assignments.

M. L. Walker and J. L. Mills (*37*), and later M. Jansen and M. Moebs (*79*), investigated the vibrational spectra of P_4O_7 (see Table XIV). In Ref. *79*, a scheme correlating the Raman-active bands of P_4O_7 with those observed in the Raman spectra of P_4O_6 and P_4O_{10} is given (see Fig. 9).

Because there is no preparative access to pure P_4O_8 (see Section II.A), no vibrational spectrum of this compound is available. The vibrational spectrum of pure P_4O_9 shows absorptions at 1379(vs), 1137(m), 989(vs), 777(m), 751(m), 657(s), 609(w), and 515(w) cm^{-1}. No assignment has yet been supplied (*121*).

2. ^{31}P NMR Spectroscopy in Solution

The ^{31}P NMR spectrum of P_4O_6 consists of an extremely narrow singlet signal (*122*); its chemical shift is $+112.5 \pm 0.1$ ppm upfield versus 85% H_3PO_4. It has been suggested to use P_4O_6 as an internal standard in ^{31}P NMR spectroscopy (*122*), becuase its resonance falls in a special region convenient for referencing the majority of phosphorus compounds. In 1979, M. L. Walker, D. E. Peckenpaugh, and J. L. Mills

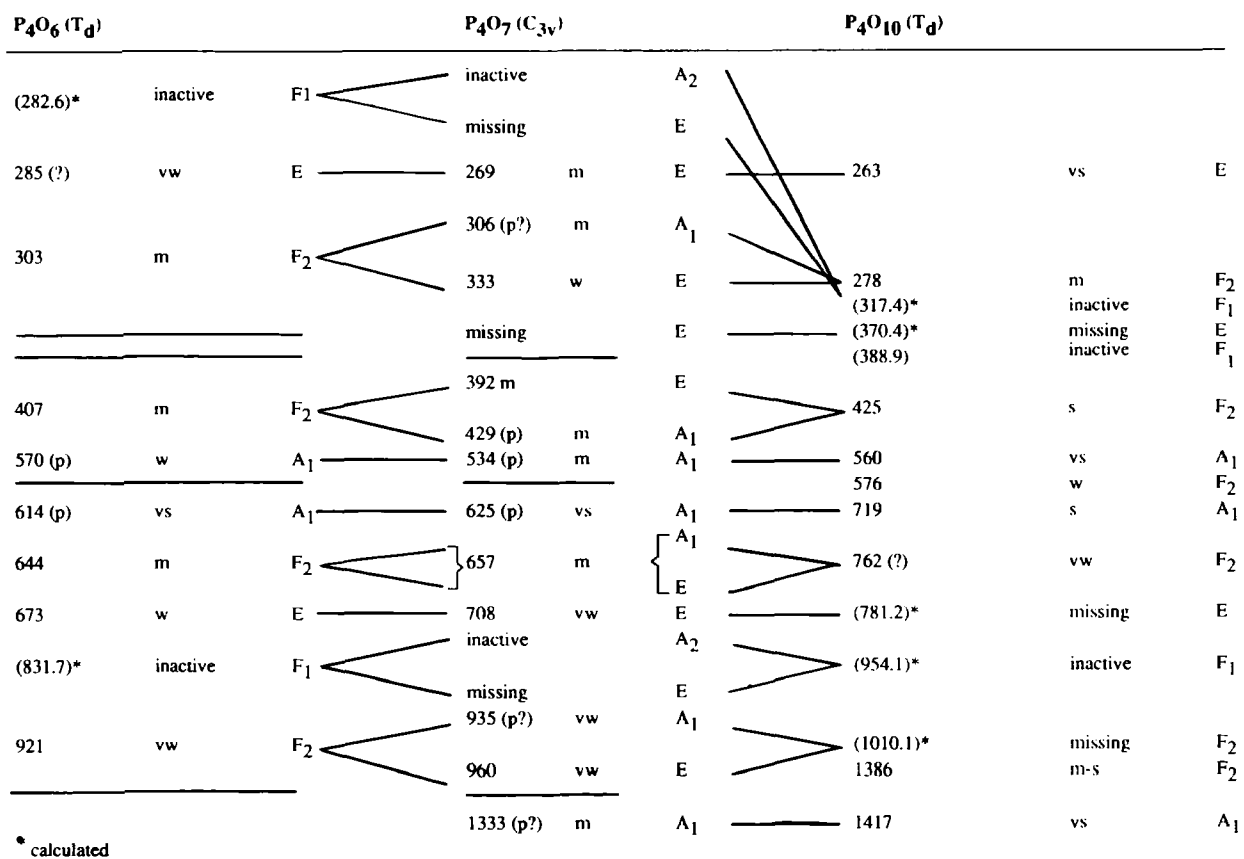

FIG. 9. Correlation of the vibrational absorption bands of P_4O_7 with those of P_4O_6 and P_4O_{10} (*79*).

TABLE XIV

IR AND RAMAN ABSORBANCES OF P_4O_7

Absorbances (37)		IR absorbances (79)			
CS_2 solution (IR)	crystalline (Raman)	CS_2 solution	crystalline	Raman lines (79)	Assignment (79)
1362(s)	1328(m)	1364(s)	1345(s)	1333(p?;m)	A_1
		1287(w)			651 · 2 = 1302
		1032(w)			424 + 629 = 1053
955(s)	958(m)	966(vs)	965(s;br)	960 (vw)	E
	928(m)	945(sh)	930(sh)	935(p?;vw)	A_1
			781(w)		392 · 2 = 784
695(m)	709(m)	696(m)	711(m)	708(vw)	E
			695(vw)		323 + 353 = 676
	677(m)		674(w)		
		{651(w)}	{667(sh), 653(w), 635(sh)}	{657(m)}	A_1
	651(m)				E
					314 · 2 = 628
627(m)	624(m)	629(m)	615(m)	625(p;vs)	A_1
			554(vw)		266 · 2 = 532
	528(m)	534(m)	532(m)	534(m)	A_1
	425(m)	424(m)	427(m)	429(p;m)	A_1
	388(m)		392(vw)	392(m)	E
			353(vw)	Missing	E
			323(w)	333(w)	E
			314(w)	Missing	E?
	303(m)		299(m)	306(p?;m)	A_1
	261(m)		266–277(m)	269(m)	E

reported their ^{31}P NMR spectroscopical investigations on phosphorus (III/V) oxide chalcogenides (*77*). They observed the resonances of P_4O_7 at +20 ppm (D) and −173 ppm (Q) and those of P_4O_8 at +11.3 ppm (T) and −154.7 ppm (T). The shifts were measured relative to P_4O_6, where positive values indicate upfield shifts. As expected from the molecular structure (see Section II.B), P_4O_7 shows an A_3X-type spin system, the resonances of the trivalent phosphorus atoms being shifted downfield. The intensity ratio of the signals (P(III)/P(V)) is 3 : 1, and the coupling constant $^2J_{PP}$ is 2.4 Hz. P_4O_8 shows an A_2X_2-type spin system; the spectrum consists of two triplet signals with an intensity ratio of 1 : 1, the coupling constant being 13.5 Hz. Because of its insufficient solubility in most organic solvents, it took until 1991 to observe the ^{31}P NMR

spectrum of P_4O_9 in solution for the first time (*82*).[7] The AX_3-type spectrum shows resonances at −56.3 ppm (Q) and −145.2 ppm (D, relative to P_4O_6), with an intensity ratio of 1 : 3. The coupling constant $^2J_{PP}$ was found to be 42.8 Hz.

3. Solid-State NMR Spectroscopy

a. P_4O_{10}. In 1991, A.-R. Grimmer and G.-U. Wolf investigated the various polymorphs of phosphorus pentoxide by means of ^{31}P MAS–NMR spectroscopy (*126*). The spectrum reported for the volatile modification suggests that in P_4O_{10} all phosphorus atoms are equivalent (which does not agree with the crystallographic features; see below). The isotropic chemical shift is +46.7 ppm (versus 85% H_3PO_4 as an external standard), and the values for the anisotropic shielding tensor are $\sigma_\perp$ = −51.7 ppm and $\sigma_\parallel$ = +244.4 ppm. This means that the shielding tensor has positive axiality along the P=O bond.[8] In an investigation (*80*), ^{31}P MAS–NMR spectra of P_4O_{10}, showing two independent isotropic signals at −45.3 and −46.9 ppm, were recorded. They corresponded to the two crystallographically independent types of phosphorus atoms (see Section II.B), with an intensity ratio of 3 : 1. The more intense of these signals has a remarkably large half width and might consist of three different signals. This would mean that all four phosphorus atoms in P_4O_{10} can be distinguished spectroscopically, whereas three of them are crystallographically equivalent (!).

b. P_4O_6. Because of the low melting point of phosphorus(III) oxide (22.8°C), solid-state NMR spectroscopy has been performed only on static samples so far (*80*).[9] The chemical shift of the isotropic P(III) signal is +113.0 ppm; the components of the anisotropic shielding tensor are listed in Table XV.

c. Phosphorus(III/V) Oxides. The ^{31}P MAS–NMR spectrum of P_4O_7 (*80*) shows two isotropic signals, at +128.1 ppm [P(III)] and −53.2 ppm [P(V)], with an intensity ratio of 2 : 1. This means that—in contrast to P_4O_{10} (see above)—the three crystallographically independent [P(III)] atoms cannot be distinguished. The remarkably large half width of the P[III] signal is probably caused by a dynamic effect, e.g., a rotation of

[7] M. L. Walker and J. L. Mills (*125*) have reported the observation of a quartet signal at −6.63 ppm, $^2J_{PP}$ = 2.5 Hz, which they assumed to be caused by P_4O_9. Reference *82* clearly points out that this attribution is not reliable.

[8] The same has previously been observed in phosphoryl compounds (*127, 128*) and some phosphates (*129*).

[9] For relaxation time measurements on solid P_4O_6 and a discussion of relaxation mechanisms, see Refs. *130, 131*.

TABLE XV

OBSERVED AND CALCULATED [IGLO METHOD (*130*)] COMPONENTS OF THE ANISOTROPIC SHIELDING TENSORS OF PHOSPHORUS OXIDES

	P_4O_6	P_4O_7	P_4O_9	P_4O_{10}
P(III)				
σ_{11} (obs)	−230	−235	−150	
(calc)	−202	−218	−151	
σ_{22} (obs)	−230	−235	−150	
(calc)	−202	−203	−151	
σ_{33} (obs)	+120	+86	+137	
(calc)	+139	+124	+146	
σ_{iso} (obs)	−113	−128	−55	
(calc)	−88	−99	−52	
P(V)				
σ_{11} (obs)		−35	−59	−52
(calc)		−41	−63	−49
σ_{22} (obs)		−35	−59	−52
(calc)		−41	−49	−49
σ_{33} (obs)		+229	+222	+244
(calc)		+240	+244	+255
σ_{iso} (obs)		+53	+35	+46
(calc)		+53	+44	+52

the molecule around its C_3 axis. Therefore only the mean values of the anisotropic chemical shift could be observed. Obviously, this effect did not affect the determination of the crystal structure by means of X-ray diffraction (see Section II.B). This suggests that the rotation proceeds via very fast rotational jumps between long stationary times. Low temperature measurements on P_4O_7 have not been performed yet.

The spectrum of P_4O_9 (*80*) shows two isotropic signals, at +54.5 ppm [P(III)] and −34.7 ppm [P(V)]. Because all three P(V) atoms are crystallographically equivalent, this agrees with the expectations. No solid-state NMR data for P_4O_8 have been reported (see Section II.A).

Graphical interpretations of the spectra [using the Herzfeld–Berger approximation (*133*)] yield the components of the anisotropic shielding tensors (see Table XV). Comparing the isotropic shifts of P(III) in P_4O_6 and P_4O_7, it becomes obvious that mainly σ_{II} is influenced by the oxidation of one single phosphorus atom, whereas $\sigma_{\perp}$ remains approximately constant. Similarly, by comparing the isotropic shifts of P(V) in P_4O_7 to P_4O_9, it is seen that mainly $\sigma_{\perp}$ is affected. These tendencies are shown in Fig. 10, in which the static spectra of the phosphorus oxides are depicted schematically.

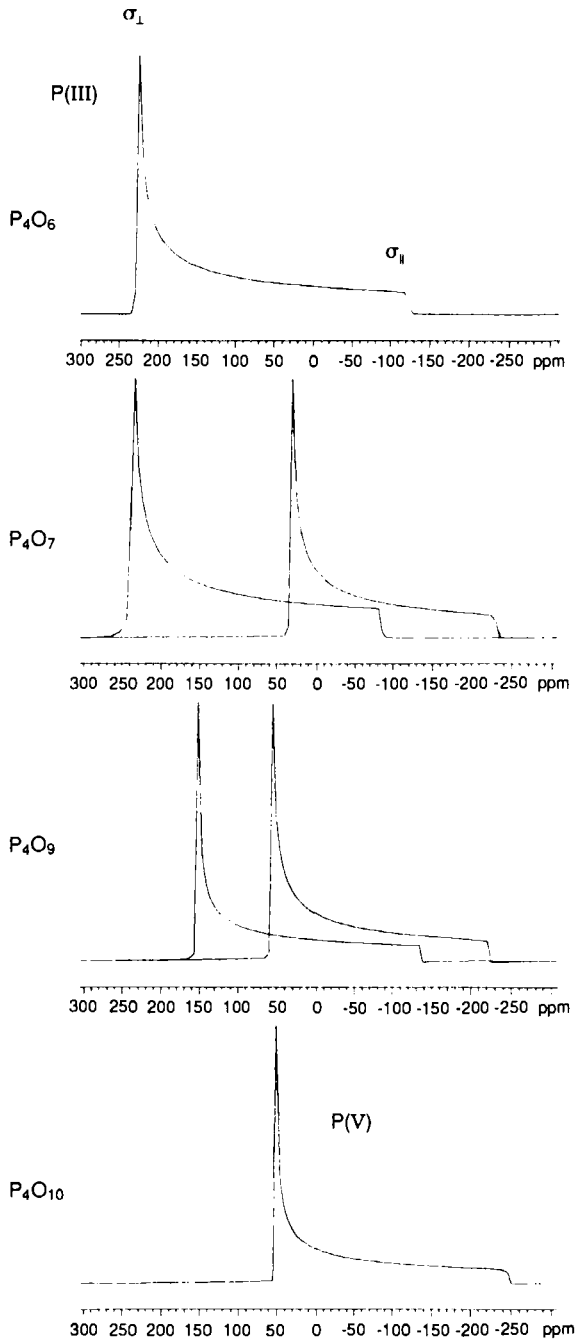

FIG. 10. Schematic representation of the ^{31}P shielding tensors of phosphorus oxides (*80*).

4. *X-Ray Absorption Spectroscopy*

The phosphorus K shell photoabsorption spectra (XANES and EXAFS) of P_4O_6 and P_4O_{10} have been reported in comparison with those of $P(OPh)_3$ and $O{=}P(OPh)_3$ (*82, 134, 135*). The absorption bands and their assignments are listed in Table XVI, and the full spectra are depicted in Figs. 11 and 12.

The first very intense absorption band at low energies (so-called "white line"; attributed to transitions of a P(V)-1*s* electron to unoccupied molecular or Rydberg-type orbitals) occurs in P_4O_{10} at 2151.74 eV, a value that is 4.30 eV higher than the energy of the white line in the spectrum of P_4O_6. This shift is explained by the higher oxidation state of phosphorus in P_4O_{10}, which implies a stronger attraction of the electrons.

The locations of the preedge absorptions and of the shape resonances of both spectra on the energy scale are very similar to those found in triphenylphosphite and triphenylphosphate, respectively. This illustrates that transistions of core electrons are mainly influenced by effects of the first coordination shell. In general, the location of the white line is characteristic for the local environment of the atom under consideration.

TABLE XVI

EXPERIMENTAL AND THEORETICAL ABSORPTION STRUCTURE FOR P_4O_6 AND P_4O_{10} (*135*)

Peak No.	Energy[a] (eV)	Term value (eV)		Assignment	Lorentz width (eV)	Peak area (*N*)	*p* density (*N*)
		Experimental	Calculated				
P_4O_6							
1	2144.57	−9.25		?	0.82	0.02	
2	2147.44	−6.25	−6.25	$1s \rightarrow 5e + 5a_1$	0.71	1	1
3	2149.7	−3.98	−3.61	$1s \rightarrow 6e$	0.9	0.3	0.81
4	2152.09	−1.60	−3.6	$1s \rightarrow 7e$	3.09	0.85	0.27
IP	2153.7	0					
5	2154.7	1		Shape resonance			
6	2164.1	9.4		Shape resonance			
P_4O_{10}							
1	2150.3	−5.87	−5.61	$1s \rightarrow 6a_1$	0.8	0.03	0.03
2	2151.7	−4.38	−4.38	$1s \rightarrow 6e$	0.93	1	1
3	2153.51	−2.97	−2.75	$1s \rightarrow 8e$	1.74	0.37	0.3
4	2154.76	−1.07	−2.07	$1s \rightarrow 9a_1 + 7e$	1.65	0.3	0.6
IP	2156.17	0					
5	2158.1	1.93		Shape resonance			
6	2161.99	5.83		EXAFS oscillation			
7	2170.17	14		Shape resonance			

[a] The energy values have been obtained by "unfolding" the spectra by a least-squares fit using Voigt profiles, the main criterium being the minimization of the number of profiles.

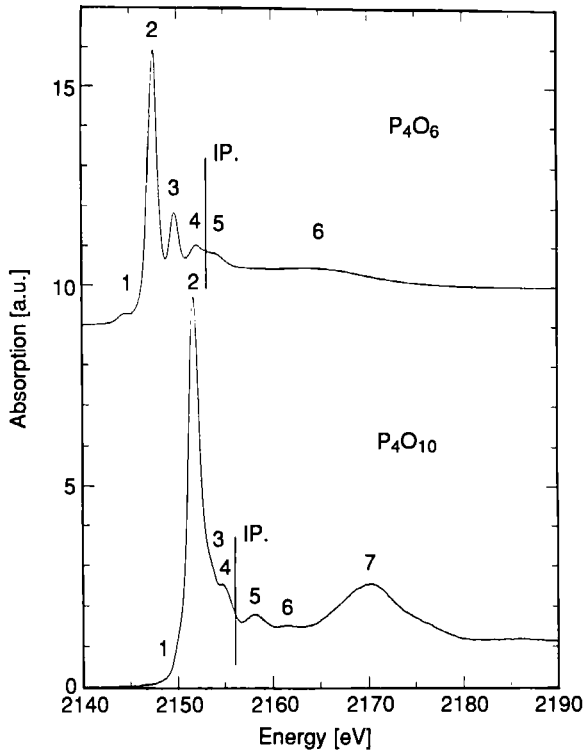

FIG. 11. XANES spectra of P_4O_6 and P_4O_{10} (*135*).

Ionization limits cannot be inferred from photoabsorption spectra; however, they are accessible from photoelectron spectra (see below). Because there exists a linear correlation between 1*s* and 2*p* binding energies, the 1*s* ionization potentials for P_4O_6 and P_4O_{10} were estimated using data reported for PCl_3 (*135*). In the case of P_4O_{10}, recent work (*138, 139*) shows that the estimated value is in excellent agreement with the experimentally determined one (see below).

The various absorption lines have been assigned with the help of MS-Xα calculations. Because the main influence on the shape of the XANES spectra is from the atoms in the first neighbor shell, only "constituent clusters" have been treated in the simulations, e.g., PO_3^{3-} for P_4O_6 and PO_4^{3-} for P_4O_{10}. In terms of this approximation, some details of the spectra (e.g., intensity and line widths of the absorptions) could be simulated sufficiently, whereas the predicted term values calculated for transitions near the absorption edge lie too close to each

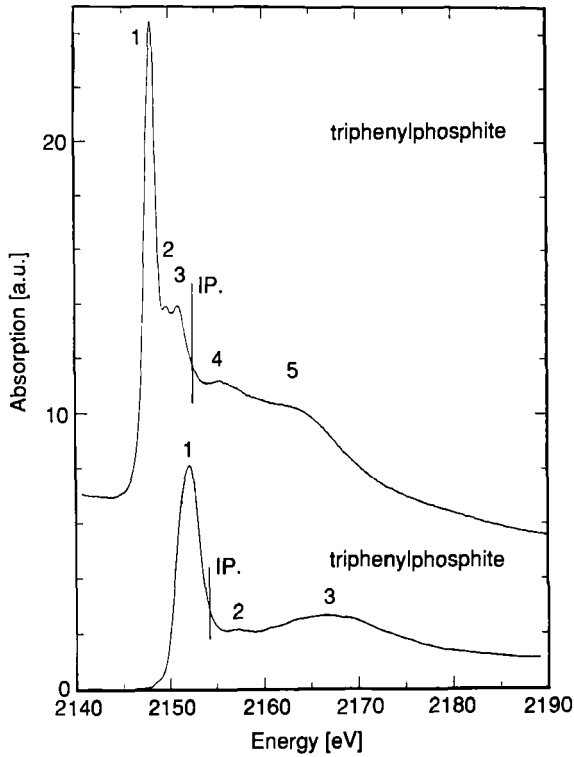

FIG. 12. XANES spectra of $(PhO)_3P$ and $(PhO)_3PO$ (*135*).

other. This points to the difficulties in modeling near-edge unoccupied orbitals (see Section II.D). The Fourier-transformed EXAFS spectra (*135*) (depicted in Figs. 13 and 14) show maxima at 1.7 and 2.95 Å (P_4O_6) and at 1.6 and 2.9 Å (P_4O_{10}), the first maximum corresponding to the P–O distance and the second corresponding to the P–P distance (the two different P–O distances in P_4O_{10} are not resolved). This is in satisfactory agreement with X-ray structural data (see Section II.B).

Besides structural information (which is of minor interest in this case), EXAFS spectra reveal experimental scattering phases for the P–O system and allow us to distinguish between resonances caused by single scattering processes and those caused by multiple scattering processes (so-called shape resonances).

If one plots the inverse squared bond lengths vs the term values of the shape resonances, a linear relation results (see Table XVII and Fig. 15), and thus an empirical correlation between the term values of

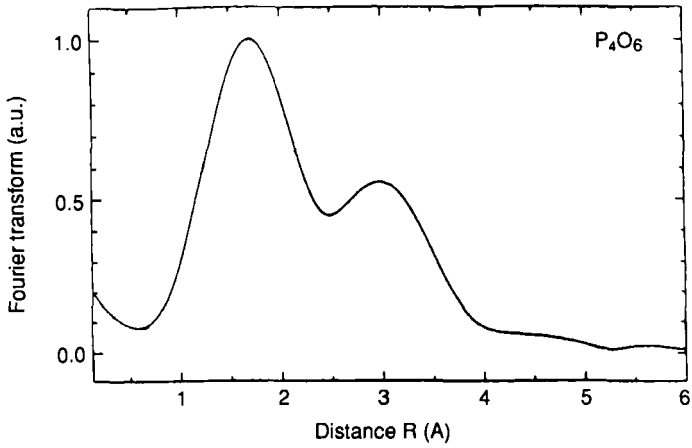

FIG. 13. Fourier-transformed and phase-corrected EXAFS spectra of P_4O_6 (*135*).

the shape resonances and the interatomic distances seems to exist (*135*). However, it is hard to find a physically meaningful explanation for the existence of this correlation.

The XANES spectrum for P_4O_9 (*80, 140*) shows a preedge absorption band at 2148.2 eV, which is assigned to an electron transition from the P(III)-1*s* orbital into an unoccupied MO with main contributions from P(III) and O. Above 2150 eV, two broad resonances have been observed, which could be fitted by three Voigt profiles of approximately

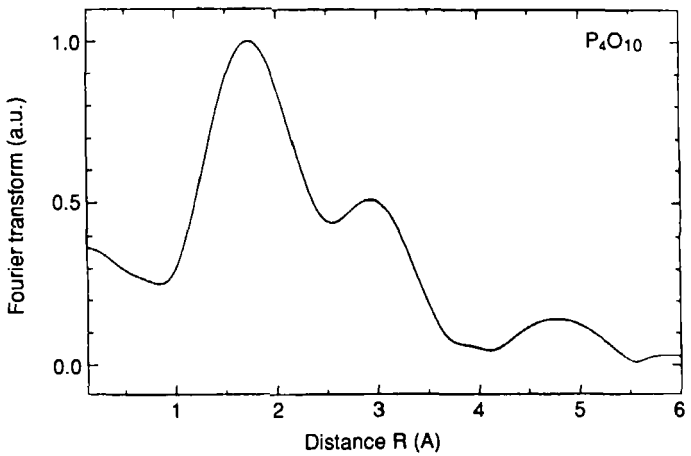

FIG. 14. Fourier-transformed and phase-corrected EXAFS spectra of P_4O_{10} (*135*).

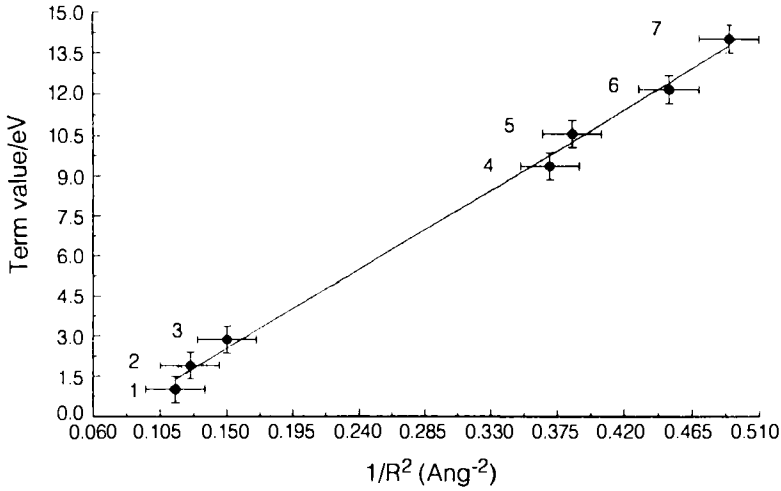

FIG. 15. Term values of the shape resonances versus the inverse squared distances (*135*).

equal amplitude and half width (at 2150.9, 2152.3, and 2153.2 eV). Comparing this part of the spectrum to the corresponding energy region of the spectrum of P_4O_{10}, these resonances can be assigned to P(V)-1*s* transitions. The "splitting" (P_4O_{10} shows only one resonance in this region; see Table XVI) is probably due to the lower symmetry of the molecule. The spectrum of P_4O_7 is rather similar to that of P_4O_6 but shows an additional absorption band at 2152.8 eV, corresponding to the excitation of an P(V)-1*s* electron. As one would expect, the intensity ratio of the P(III)/P(V) absorption bands is 3 : 1, whereas it is 1 : 3 in the case of P_4O_9.

TABLE XVII

TERM VALUES OF THE SHAPE RESONANCE AND DISTANCES (*135*)

Molecule	Distance (Å)	$1/r^2$ (Å^{-2})	Term value [eV]	No.
P_4O_6	P—P = 2.95	0.115	1	1
P_4O_{10}	P—P = 2.826	0.125	1.9	2
$P(OC_6H_5)_3$	P—C = 2.582	0.15	2.86	3
$PO(OC_6H_5)_3$	P—C = 2.582	0.15	2.84	3
P_4O_6	P—O = 1.647	0.37	9.4	4
$P(OC_6H_5)_3$	P—O = 1.61	0.385	10.6	5
$PO(OC_6H_5)_3$	P=O = 1.49	0.45	12.2	6
P_4O_{10}	P=O = 1.44	0.49	14.0	7

TABLE XVIII

IONIZATION ENERGY DATA FOR P_4O_6 (*141*)

IE [eV]	Assignment
10.55	$5t_2$ (P lone pair)
12.79	$3a_1$ (P lone pair)
	$2e$ (P—O bonding)
	$2t_1$ (O lone pair)
13.90	$4t_2$ (O lone pair)
15.84	$3t_2$ (P—O bonding)
17.98	$1t_1$ (P—O bonding)
	$2a_1$ (P 3*s*)
21.71 [He(II)]	$2t_2$ (P 3*s*)

5. *Photoelectron and Auger Electron Spectroscopy*

UV photoelectron spectra of P_4O_6 and P_4O_{10} have been reported (*141*) and compared with the spectrum of P_4 (*142, 143*). The He(I) photoelectron spectrum of P_4O_6 contains five well-defined bands; an extra band

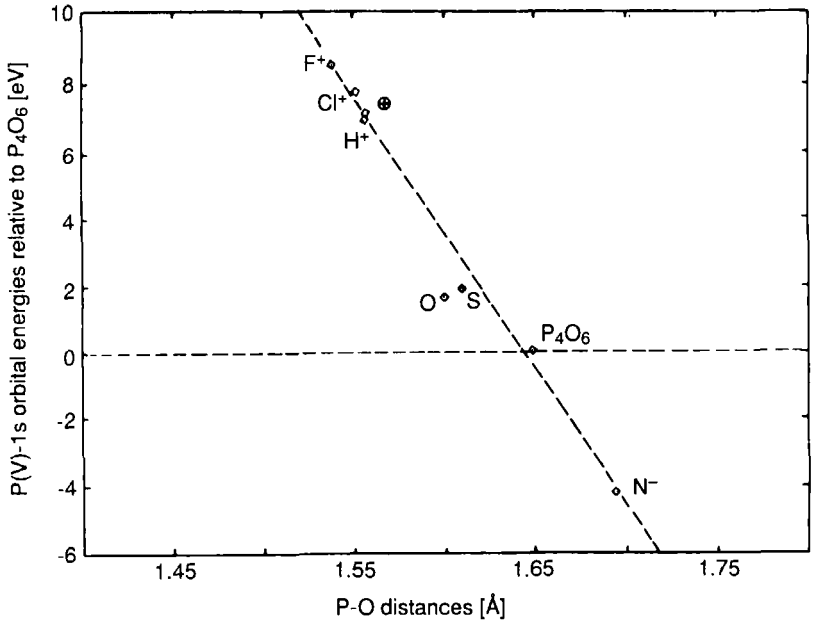

FIG. 16. Correlation of the 1s energies of P(V) with the P(V)—O_b bond lengths for P_4O_6 derivates (*165*).

TABLE XIX

IONIZATION ENERGY DATA FOR P_4O_{10} (*141*)

IE (eV)	Assignment
13.40	$3t_1$ (apical O pπ)
13.92	$7t_2$ (apical O pπ)
14.44 (sh)	$3e$ (apical O pπ)
14.76 (sh)	$6t_2$ (O lone pair)
15.36	$6t_2$ (O lone pair)
	$2e$ (P—O bonding)
	$4a_1$ (P lone pair)
16.54	$5t_2$ (O lone pair)
18.37 [He(II)]	$4t_2$ (P—O bonding)
20.80 [He(II)]	$1t_1$ (P—O bonding)
	$3a_1$ (P 3*s*)
23.83 [He(II)]	$3t_2$ (P 3*s*)

appears at a higher binding energy in the He(II) spectrum. Due to the more complicated electronic structure of P_4O_{10}, its UPS bands are more difficult to assign. However, a clear qualitative resemblance to the spectrum of P_4O_6 in the high-binding-energy region is observed, and the experimental ionization energies of both oxides (see Tables XVIII and XIX) have been correlated with each other (and with those of P_4) (*141*) (see Fig. 16). These experimental results are in excellent agreement with *ab initio* MO calculations (*141*).

X-ray photoelectron spectroscopy (XPS) has been used to determine phosphorus (and oxygen) core binding energies in P_4O_6 (*144*) and P_4O_{10} (*145–147*). The energy values obtained are listed in Table XX. As in

TABLE XX

CORE BINDING ENERGIES OF P_4O_6 AND P_4O_{10} (eV)

	P(1s)	P(2s)	P(2p)	O(1s)	Ref.
P_4O_6			139.87	539.25(3)	*148*
P_4O_{10}			137.4		*147*
			Experimental 135.6	534.2	*144*
				532.5	
			Theoretical 139.3	517.3	
				515.0	
	2150.25	193.25	135.8		*138, 139*

the case of the UPS spectra (see above), the values for P_4O_{10} are in sufficient agreement with MS-Xα calculations of the electronic structure. The most prominent peak in the Auger electron spectrum of P_4O_{10} was observed at 1848.0 eV ($KL_{2,3}\,L_{2,3}$; $^1D_2$). With respect to the XPS data listed in Table XX, the Auger parameters α = 1983.8 eV, ξ = 30.65 eV, and R_s^{ea} (2p2p) = 6.55 eV are obtained (*135, 136*).

6. *Other Techniques*

The vacuum-ultraviolet spectrum of P_4O_6 (*149*) shows two bands at ~48900 cm^{-1} and 63900 cm^{-1}, the first of which exhibits a low-energy shoulder. By analyzing the energies of these bands with respect to the symmetry of the molecule, they can be assigned to fully allowed $^1A_1 \rightarrow {}^1T_2$ transitions (mainly involving orbital transitions $5t_2 \rightarrow 3e$ and $2t_1 \rightarrow 3e$, respectively). The experimentally obtained data are reproduced by extended Hückel and *ab initio* SCF calculations.

The microwave spectrum of the pyrolysis products of CH_3OPCl_2 in the range of 26.5–39.5 GHz (*150*) suggests that—in addition to $CH_2{=}PCl$, $HC{\equiv}P$, CH_3Cl, and HCHO—P_4O_7 is present. This assumption is based on the observed rotational constant of the molecule (B_{obs} = 827.8).

Mass spectrometric studies on P_4O_{10} and P_4O_6 have been conducted (*151, 153*). In Ref. *151*, thermodynamic properties of P_4O_{10} are derived and compared with earlier data (for example, Refs. *156–159*), and in Ref. *153*, the heat of formation of P_4O_6 is derived by measuring the temperature dependence of the equilibria by mass spectrometry (H_f = -405 ± 17 kcal/mol). This latter value for the heat of formation of P_4O_6 seems to be in good accordance with that reported by S. B. Hartley and J. C. McCoubry (*160*), whereas the data given by W. R. Koerner and E. Daniels deviate considerably (*161*). The mass spectra indicate that all three phosphorus(III/V) oxides can exist in the vapor phase; the fraction of the lower oxides increases with higher temperatures.

D. Theoretical Studies

1. *General Remarks*

Only a few theoretical studies on molecular phosphorus oxides have been reported, with broadly differing purposes. Two investigations deal with the explanation of photoelectron data and core binding energies (*141, 148*), whereas in a third UV, vacuum-UV, and MCD spectra (*149*) are considered. The results of MS-Xα calculations have been compared to XANES spectra (*135*), and IGLO calculations served to simulate MAS–NMR spectra (*162*). The only substances considered were P_4O_6 and P_4O_{10}. Some calculations referring directly to data obtained from

spectroscopic investigations were mentioned in Section II.C, whereas the literature reviewed in this section is of a more general scope.

2. Bonding Features

The goal of an early publication (*163*) was to investigate the extent to which the formally empty 3*d* orbitals of phosphorus participate in the bonding scheme of P_4O_6 and of P_4O_{10}. For these calculations of the LCAO SCF CNDO formalism has been used. Population analyses demonstrated that 3*d* orbital participation should occur to a considerable degree. The *d*-orbitals are notably occupied, and their populations increase with an increasing number of oxygen atoms in the molecule. It has been suggested that electronegative groups attached to the phosphorus atoms would lead to a contraction of the 3*d* orbitals and cause them to mix with the inner orbitals (*s, p*) to a greater extent. Moreover, P_4O_6 appears to be virtually nonpolar, whereas in P_4O_{10} the P–O_t bonds are highly polarized. They are found to be multiple in nature and to have a considerable π component involving the *p* and *d* orbitals on phosphorus. However, subsequent investigations have shown that semiempiric calculations (for example, CNDO)—in contrast to *ab initio* methods—are not reliable for atoms beyond the second period, because the fixing of the parameters for *d*-AOs is problematic (*164*). Mulliken population analyses and determinations of the orbital energies in P_4O_7 have been compared with those for P_4O_6S (see Section III.D) (*166*).

An explanation was attempted for the geometrical distortion of the P_4O_6 cage when an oxygen or sulfur atom is added (*165*). The geometries of the molecules P_4O_6 and P_4O_7 (P_4O_6S) were calculated using a DZP-based HF formalism and were found to be in an excellent agreement with experimental data. Moreover, the geometries of other hypothetical P_4O_6 derivatives [$P_4O_6^+$ and P_4O_6X ($X = F^+, Cl^+, H^+, N^-$)] have been determined. The calculated P(V)–O_b distances of these molecules are correlated with the effective charges on the P(V) atoms (see Fig. 17). As a measure for the effective charges, the P(V)-1*s* energy shifts (compared with the 1*s* energy of phosphorus in P_4O_6) have been used. The P(V)–O_b distances in the different P_4O_6 derivatives vary over a range greater than 15 pm, and in the case of $P_4O_6N^-$ the bond length would even increase compared with P_4O_6.

The distances of P(V)–O_b have been plotted vs the distance of P(III)–O_b. Although the substituent X is changed, the sum of these two bond lengths remains approximately constant. The general conclusion from this work is that the geometrical distortion of the P_4O_6 cage as a whole can be related to the amount of charge transferred to the terminal substituent (*165*).

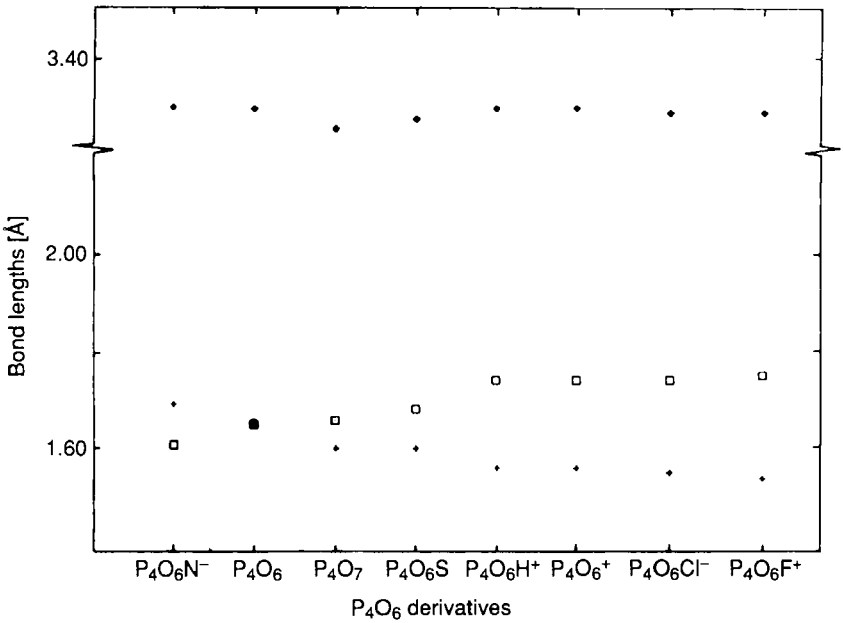

FIG. 17. Bond lengths of P(V)—O_b (+), those of P(III)—O_s (□), and sum of both (◆) for P_4O_6 derivates.

III. Molecular Phosphorus Oxide Sulfides

A. SYNTHESES

1. General Remarks

Two general routes for the preparation of phosphorus oxide sulfides are reported in the literature:

—Sulfurization of phosphorus oxides (route 1) and
—Commutation reaction between P_4O_{10} and P_4S_{10} (route 2).

The preparative challenge in both cases is the exact adjustment of the experimental parameters in order to obtain the desired species as the major product.

2. Phosphorus(V) Oxide Sulfides

a. Historical Aspects. Until 1976, $P_4O_6S_4$ was the only phosphorus oxide sulfide identified unambiguously. It was first mentioned in 1891

by T. E. Thorpe and A. E. Tutton (*3, 4*), who heated a sealed tube containing P_4O_6 and S to 168°C. A very vigorous reaction was observed, and the authors noted that the use of more than 5 g of P_4O_6 and its equivalent of sulfur led to a violent explosion. In 1897, a compound of the composition $P_4O_4S_6$ was reported to form during the reaction of $POCl_3$ with H_2S (*167*). Only elemental analyses were available to confirm the composition. $P_4O_4S_6$ is also supposed to form by the reaction (*168*)

$$6(CH_3)_3SiSSi(CH_3)_3 + 4\,POCl_3 = 12(CH_3)_3SiCl + P_4O_4S_6.$$

Elemental analysis (sulfur content) was the only evidence given for the existence of this oxide sulfide, and a speculative structure analogous to P_4O_{10} with the six bridging atoms of the cage being sulfur atoms, was proposed. However, J. L. Mills and coworkers (*77*) were not able to reproduce the syntheses as reported and concluded that the structure suggested for $P_4O_4S_6$ was at least unlikely. In addition, the melting point as reported by E. W. Abel *et al.* differs from that obtained by G. U. Wolf and M. Meisel, who proved the identity of their product ($P_4O_4S_6$) unambiguously (see below).

b. Preparation according to Route 1. In 1973, a patent (*169*) describing a continuous technical process for the preparation of $P_4O_6S_4$ from P_4O_6 and S was applied for. In this process, P_4O_6 is added to a sulfur melt heated at 190°C, and so the limitations of the method of Thorpe and Tutton were overcome. $P_4O_7S_3$ and $P_4O_8S_2$ have been detected as by-products in the reaction of P_4O_7 and P_4S_{10} in *o*-xylene (*77, 170*).

c. Preparation according to Route 2. The use of the reorganization reaction is the preferred route for preparing $P_4O_6S_4$ because the starting materials are easily available. P_4O_{10} and P_4S_{10} are mixed in a molar ratio of 3 : 2 and then heated at 400°C for a few hours. $P_4O_6S_4$ is distilled from the reaction mixture simultaneously with its formation therein (*171, 172*). Other phosphorus(V) oxide sulfides can be prepared by the reaction of P_4O_{10} and P_4S_{10} in a P_4S_{10}/sulfur melt at 500°C (*173*). $P_4O_5S_5$ and $P_4O_4S_6$ are obtained as pure substances by repeated distillation *in vacuo* of the products that continuously distill off the mixture during the reaction. P_4OS_9 can be obtained in a pure state by extraction of the distillation residue with CS_2 and subsequent evaporation of the solvent. $P_4O_8S_2$, $P_4O_7S_3$, $P_4O_3S_7$, and $P_4O_2S_8$ are available only as mixtures and have been identified by ^{31}P NMR spectroscopy in solution (*173*).

3. *Phosphorus(III/V) Oxide Sulfides*

a. Historical Aspects. The oxidation of P_4S_3 in CS_2 solution with molecular oxygen has been found to yield an amorphous phosphorus oxide sulfide of the composition $P_4S_3O_4$ (*174*). The substance was characterized by elemental analysis, and the authors thought to have obtained a compound analogous to the phosphorus sulfide P_4S_7. However, until 1976 (*170*) no phosphorus(III/V) oxide sulfide was definitely known.

b. Preparation according to Route 1. Pure P_4O_6S and pure $P_4O_6S_2$ are accessible by reacting P_4O_6 with P_4S_{10} in toluene or *o*-xylene, respectively (*77, 170, 175*). P_4O_7S, $P_4O_7S_2$, and P_4O_8S have been detected spectroscopically (^{31}P NMR) among the product mixtures resulting from the reaction of P_4O_7 and P_4S_{10} in *o*-xylene (*77, 170*).

c. Preparation according to Route 2. Pure $P_4O_3S_6$ forms analogously to P_4OS_9 (see above) by fractional crystallisation from a CS_2 solution that is obtained by extraction of the solid residual products from the reaction of P_4O_{10} and P_4S_{10} (*173*).

d. Preparation of $P_4O_6S_3$. Pure $P_4O_6S_3$ can be prepared by desulfurization of $P_4O_6S_4$ with $P(C_6H_5)_3$ in toluene at room temperature (*175*).

B. Crystal and Molecular Structures

1. *Crystal and Molecular Structure of $P_4O_6S_4$*

The molecular structure of $P_4O_6S_4$ in the gaseous state was determined in 1939 by means of electron diffraction (*176*). Its crystal structure was determined by X-ray diffraction (*177*) and refined on the basis of diffractometer data in order to obtain state-of-the-art structural parameters (*80*). The bond lengths and angles obtained in these three investigations are listed in Table XXI.

TABLE XXI

Molecular Structure of $P_4O_6S_4$

	Ref. *176*	Ref. *177*	Ref. *80*
Distance P(V)—O_c	1.61(2) Å	1.62(2) Å	1.620(2) Å
Distance P(V)—S	1.85(2) Å	1.86(2) Å	1.886(1) Å
Angle O_c—P(V)—O_c	101.5(1.0)°	100.8(9)°	101.7(1)°
Angle O_c—P(V)—S	123.5(1.0)°	117.2(8)°	116.7(1)°
Angle P(V)—O_c—P(V)	116.5(1.0)°	124.5(6)°	124.2(3)°

Note. Standard deviations are given in parentheses.

TABLE XXII

BOND LENGTHS (Å) IN PHOSPHORUS OXIDE SULFIDES (*80*)

	P_4O_6S	$P_4O_6S_2$	$P_4O_6S_3$	$P_4O_6S_4$
P(III)—O_a	1.637(2)	1.636(2)		
P(III)—O_b	1.678(2)	1.671(2)	1.661(2)	
P(V)—O_b	1.596(2)	1.595(2)	1.595(2)	
P(V)—O_c		1.614(2)	1.611(2)	1.620(1)
P(V)—S	1.890(1)	1.885(1)	1.882(1)	1.886(1)

Note. Standard deviations are given in parentheses.

2. *Crystal Structure of $P_4O_3S_6$*

Among the structurally characterized phosphorus oxide sulfides, $P_4O_3S_6$ is the only representative that is not derived from the P_4O_6 cage (*178, 179*). Its molecular structure is shown in Fig. 18. The structure is analogous to that of P_4O_9 (see above), with three oxygen and three sulfur atoms bridging the four phosphorus atoms in the adamantane-like cage, as well as three terminally bonded sulfur atoms.

3. *Crystal Structures of $P_4O_6S_n$ (n = 1–3)*

The structures of pure P_4O_6S, $P_4O_6S_2$, and $P_4O_6S_3$ in the solid state were determined (*166, 175*). The structural data obtained are listed in Tables XXII and XXIII. The P_4O_6 cage is made to contract by successive addition of sulfur atoms, as can be seen in Table XXIV, in which the

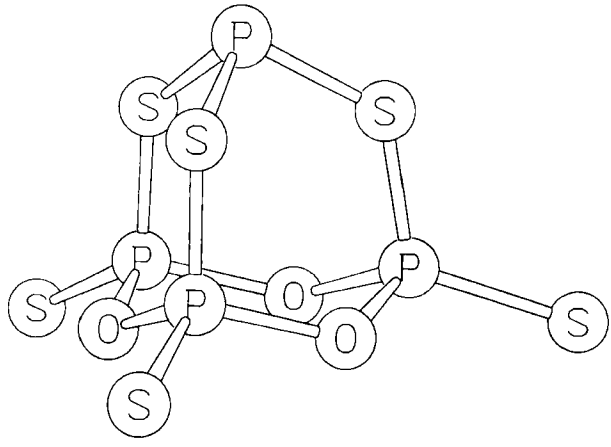

FIG. 18. Molecular structure of $P_4O_3S_6$ (*179*).

TABLE XXIII

ANGLES (°) IN PHOSPHORUS OXIDE SULFIDES (*80, 101*)

	P_4O_6	P_4O_6S	$P_4O_6S_2$	$P_4O_6S_3$	$P_4O_6S_4$
O_a—P(III)—O_a	99.6	99.5			
O_a—P(III)—O_b		98.6	98.8		
O_b—P(III)—O_b			98.0	98.4	
O_b—P(V)—O_b		103.1	103.6		
O_b—P(V)—O_c			101.5	101.6	
O_c—P(V)—O_c				100.8	101.2
O_b—P(V)—S		115.3	116.6	117.9	
O_c—P(V)—S			115.1	116.1	116.9
P(III)—O_a—P(III)		128.1	129.0		
P(III)—O_b—P(V)		124.2	125.2	126.1	
P(V)—O_c—P(V)			123.5	124.2	124.2

volumes of the cages of the different substances are compared with each other.

By comparing the molecular geometries of the phosphorus oxide sulfides with those of the oxides, it is obvious that the extent of the distortion due to binding terminal chalcogen atoms depends on whether oxygen or sulfur is added. In the $P_4O_6S_3$ molecule, the P(V)–O_b distance is shorter than that in the corresponding oxide, P_4O_9. This produces a discrepancy in the results obtained from an analogous consideration of the P_4O_7 and P_4O_6S moelcules, for which the geometries of the P_4O_6 cages remain virtually identical (*166*). As with the oxides, the molecules of the phosphorus oxide sulfides in the solid state belong, within the limits of experimental error, to the same point group that would be expected for the free molecules (*80, 166, 175*).

TABLE XXIV

VOLUMES OF THE P_4O_6 CAGES OF THE SUBSTANCES $P_4O_6S_n$ (n = 0–4) (*80*)

Substance	Volume of the P_4O_6 cage (Å^3)
P_4O_6	100.7
P_4O_6S	99.8
$P_4O_6S_2$	98.9
$P_4O_6S_3$	96.9
$P_4O_6S_4$	96.1

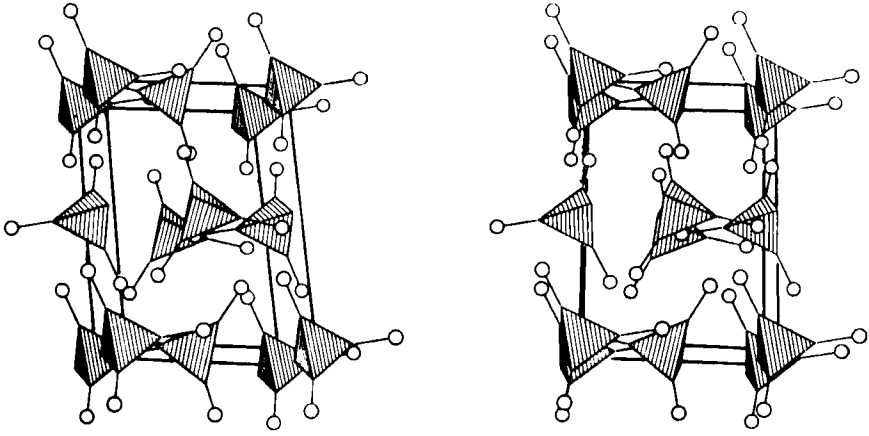

FIG. 19. Stereoplot of the unit cell fo $P_4O_6S_3$ (shifted by 0.2442; 0.0248; 0.3283) (*175*).

4. Molecular Packings of the Phosphorus Oxide Sulfides $P_4O_6S_n$ (n = 0–4) in the Solid State

In contrast to the oxides, the phosphorus oxide sulfides do not show pronounced relationships to each other with respect to their metrices or space group symmetries. The P_4O_6S and $P_4O_6S_3$ molecules form a severely distorted face-centered cubic packing (*166, 175*). This is shown for $P_4O_6S_3$ in Fig. 19 (the P_4O_6 cages are representated by tetrahedra). The section shown has its origin shifted by 0.2442; 0.0248; 0.3283.

For $P_4O_6S_2$, no simple description for the molecular packing has been found. $P_4O_6S_4$ molecules form a slightly distorted primitive cubic packing, as can be seen in Fig. 20 (*80*).

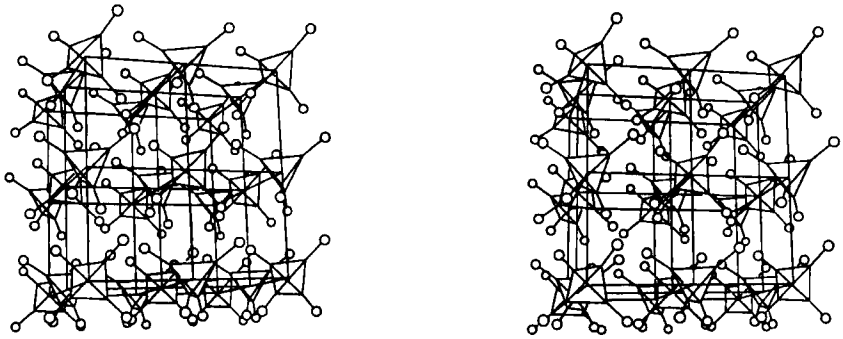

FIG. 20. Stereoplot of the packing of $P_4O_6S_4$ molecules (*80*).

TABLE XXV

PACKING OF $P_4O_6X_n$ MOLECULES (X = O, S; n = 0–4) IN THE SOLID STATE (*80*)

	P_4O_6	P_4O_6S (P_4O_7)	$P_4O_6S_2$	$P_4O_6S_3$ (P_4O_9)	$P_4O_6S_4$ (P_4O_{10})
Density (g/cm^3)	2.14	2.21 (2.34)	2.23	2.10 (2.64)	2.05 (2.28)
Molar volume (cm^3)	99.3	114.0 (100.8)	127.4	150.5 (101.5)	175.6 (123.0)
Volume of the molecule (Å^3)	100.7	117.15 (103.5)	135.9	152.9 (109.4)	171.5 (110.2)
Volume of the unit cell/Z (Å^3)	164.9	189.5 (166.3)	211.2	250.6 (168.6)	282.7 (207.0)
Efficiency value	0.61	0.62 (0.62)	0.64	0.61 (0.65)	0.61 (0.53)

The occurrence of completely different crystal structures within the same class of substances, as well as the difference in the structures of the analogous oxides, is surprising, especially if one is aware that van der Waals-type forces are predominant in all cases. Achievement of an effective space-filling is thought to be the main factor determining the type of a molecular van der Waals packing. It has been shown for many structures of organic compounds that the principle of "dovetailing" ("protrusions" into "hollows") is effective (*106*). In order to check whether this principle applies in this case, the volumina of the $P_4O_6X_n$ molecules are compared in Table XXV with the space available in the respective crystal lattice (*80*), which is obtained by dividing the volume of the unit cell by the number of molecules in it. The ratio of the two volumina is defined as the "efficiency" of the packing.

With the exception of P_4O_{10}, efficiency values between 0.61 and 0.65 have been obtained. This indicates that, in spite of the differences among the crystal structures of the phosphorus oxides and oxide sulfides, their space-fillings are very similar.

C. SPECTROSCOPY

1. Vibrational Spectroscopy

a. $P_4O_6S_4$. Characterizations of $P_4O_6S_4$ by means of vibrational spectroscopy (*180*) have resulted in a complete assignments of the absorption bands observed, as well as force constant calculations (*108*). Table XXVI summarizes these early data and compares them to later

TABLE XXVI

VIBRATIONAL ABSORPTION BANDS OF SOLID $P_4O_6S_4$

Ref. *180*	Ref. *113*		Ref. *80*		Assignment
Ra	Ra	IR	Ra	IR	*113*
				1388(m)	
				1328(m)	
				1214(m)	
				1139(w)	
		981		978(vs)	F_2
934(p)	930		929(w)		A_1
	897		898(vw)	882(m)	E
		769		753(w)	F_2
			713(vw)	712(w)	
700(dp)	694		698(w)	704(w)	A_1
668(dp)	666		669(w)	671(s)	F_2
			646(vw)	646(m)	
				569(w)	
				548(m)	
498(p)					
		460			F_2
447(p)			447(vw)		
400(dp)	400		406(vs)		A_1
			387(m)		
354(dp)	353		352(m)		F_2
			328(w)		
			317(vw)		
			288(vw)		
			271(vw)		
	259				E
194(dp)	194				F_2
			170(w)		
			160(s)		
			155(vs)		
150(dp)	148		145(vs)		E
			133(w)		
95					

experimental data (*80*). The most reliable values for the wave numbers are those from Ref. *80*, a study in which a spectrometer with significantly higher resolution than that in the previous investigations was used. Thus in this work many more bands were observed than reported in the older literature; e.g., the Raman line at 150 cm^{-1} [already observed by H. Gerding and H. v. Brederode in 1945 (*180*)] is split into five bands at 170, 160, 155, 145, and 133 cm^{-1} due to lattice effects.

The bands at 1388 cm^{-1} might be explained by the presence of small amounts of P_4O_{10} due to the route of preparation (see Refs. *171* and *172*). Force constants for the $P_4O_6S_4$ molecule were calculated from Raman spectra and were improved later (*113*). Table XXVII gives the values obtained using the simple valence force field method (I) or the extended force field method (II) (*113*); the calculations have been carried out using interatomic distances and angles from electron diffraction data (*178*).

b. Phosphorus(III/V) Oxide Sulfides. The infrared spectrum of P_4O_6S was recorded in 1979 (*77*). However, it took until 1993 (*80*), when each compound of the series $P_4O_6S_n$ ($n = 1–3$) became available as a pure substance (see Section II.A), for comprehensive spectroscopical studies. The vibrational absorption bands of these species in a crystalline state are listed in Tables XXVIII and XXIX.

Given the molecular symmetries of the phosphorus(III/V) oxide sulfides, 16 absorption bands (both IR and Raman) for P_4O_6S (point group, C_{3v}), 25 IR and 30 Raman bands for $P_4O_6S_2$ (point group, C_{2v}), and 19 bands (both IR and Raman) for $P_4O_6S_3$ (point group, C_{3v}) are expected. All IR-active absorptions should be Raman active too. Deviations of the expected spectra from the observed spectra are in most cases due to the fact that symmetry analyses do not predict the intensity of an absorption band. The experimental spectra of $P_4O_6S_3$ show more than the 19 absorptions predicted from symmetry analysis. This is an indica-

TABLE XXVII

FORCE CONSTANTS [mdyn/Å] FOR THE $P_4O_6S_4$ MOLECULE (*113*)

	I	II
f (PO)	5.25	3.848
f (PS)	5.50	5.122
d (POP)	0.35	0.373
d (OPO)	0.35	0.187
d (OPS)	0.43	0.373
F_q[a]		0.12
F_s		0.69
F_t		0.08

[a] F_q, F_s, and F_t are the coefficients for the second-order development of the potential energy (see Section II.C).

TABLE XXVIII

VIBRATIONAL ABSORPTION BANDS OF P_4O_6S

Ref. *77*	Ref. *80*		Ref. *77*	Ref. *80*	
IR	Ra	IR	IR	Ra	IR
		2924(w)	528(m)		534(w)
		2853(w)	515(m)		
		1264(s)		505(s)	502(w)
		1202(w)			466(w)
1006(m)		1010(sh)			451(w)
940–986(s)	958(w)	948(s;br)	415(m)	415(m)	417(m)
895(m)	911(w)	900(sh)		344(m)	
850(m)	814(w)	830(m)		313(w)	
687(m)	690(w)	688(m)		300(m)	
663(m)		668(w)		186(s)	
642(m)	653(w)	646(w)		159(w)	
626(m)	632(m)	631(w)		59(s)	
	592(s)	598(m)		32(s)	

TABLE XXIX

VIBRATIONAL ABSORPTIONS OF $P_4O_6S_2$ AND $P_4O_6S_3$ (*80*)

$P_4O_6S_2$		$P_4O_6S_3$		$P_4O_6S_2$		$P_4O_6S_3$	
Ra	IR	Ra	IR	Ra	IR	Ra	IR
	1360(w)			498(vs)	502(s)	485(vs)	486(s)
	1286(w)			483(w)	473(vw)		
	1207(m)		1212(m)			446(m)	450(vw)
	960(vs)	951(vw)	960(vs)	420(w)	421(s)		
915(w)				367(vw)			
848(w)	849(sh)	893(w)	894(sh)	354(s)		372(s)	
	742(vw)		767(m)	343(m)		349(s)	
	728(vw)		722(w)			326(w)	
		715(vw)	713(w)	301(w)		308(w)	
		703(vw)	702(w)	290(w)		289(vw)	
675(m)	677(m)	678(m)	666(vw)	205(m)			
652(vw)	651(m)	656(vw)	652(vw)	187(vs)		198(s)	
632(m)	628(s)	638(w)	639(vs)			163(m)	
610(vw)	609(m)			159(vs)		155(vs)	
583(w)	585(w)					146(vs)	
571(m)	571(w)	568(w)	568(vw)	77(w)			
525(vw)	524(s)		536(s)	55(vs)			
				30(vs)			

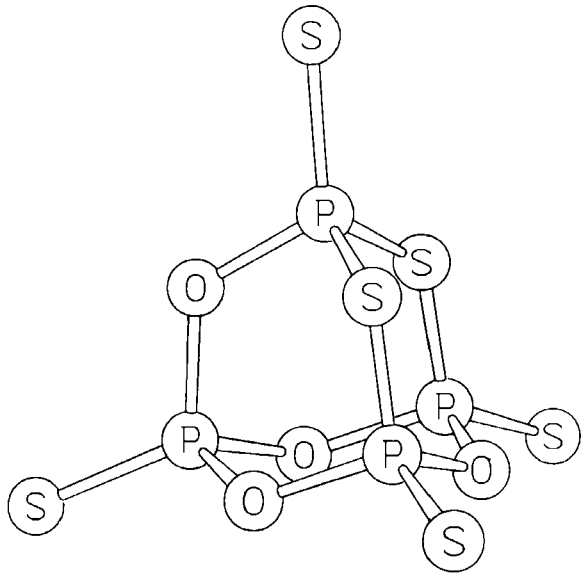

FIG. 21. Molecular structure of $P_4S_6O_4$ (*182*).

tion that the symmetry has been reduced by the effect of the crystal lattice, and therefore the point group approximation is no longer sufficient. Calculations of force constants of phosphorus(III/V) oxide sulfides are ongoing. In order to gain an experimental basis as broad as possible for the discussion of correlations between molecular geometry and chemical bonding, such calculations are very desirable.

2. *^{31}P NMR Spectroscopy in Solution*

The ^{31}P NMR spectrum of $P_4O_6S_4$ in CS_2 solution (*181*) consists of a singlet signal with a chemical shift of −103.4 ppm relative to internal P_4O_6. For $P_4O_4S_6$, H. Grunze (*182*) has reported an AX_2Y-type spectrum, which would be in agreement with the molecular structure shown in Fig. 21.

The ^{31}P NMR spectra of the remaining phosphorus oxide sulfides[10] were recorded using solutions that in most cases contained mixtures of these compounds (*77*). The chemical shifts and coupling constants

[10] The phosphorus oxide sulfide $P_4O_3S_6$ has been described by G. U. Wolf and M. Meisel (*178*) shows an A_3X-type ^{31}P NMR spectrum with signals at +46.0 ppm [P(III)] and +55.7 ppm [P(V)], the coupling constant being 108 Hz. This corresponds to the molecular structure described in Section III.B.

TABLE XXX

^{31}P NMR SPECTRA OF PHOSPHORUS (III/V) OXIDE SULFIDES IN SOLUTION WITH P_4O_6 AS THE INTERNAL STANDARD (*77*)

	P(III) δ (ppm)	P(V)=O δ (ppm)	P(V)=S δ (ppm)	$^2J_{PP}$ (Hz)
P_4O_6S	+12.5 (D)		−101.7 (Q)	12.8
$P_4O_6S_2$	+9.2 (T)		−92.3 (T)	1.9
$P_4O_6S_3$	−27.5 (Q)		−91.8 (D)	14.3
P_4O_7S	+11.0	−160.0	−88.1	9.5 [P(III)—P=O]
				0.7 [P(III)—P=S]
				46.5 (P=O—P=S)
$P_4O_7S_2$	−32.9	−155.5	−89.1	28.1 [P(III)—P=O]
				18.7 [P(III)—P=S]
				50.0 (P=O—P=S)
$P_4O_7S_3$		−159.5 (Q)	−103.2 (D)	48.0
P_4O_8S	−38.9	−152.2	−87.0	33.0 [P(III)—P=O]
				23.0 [P(III)—P=S]
				55.0 (P=O—P=S)
$P_4O_8S_2$		−159.0 (T)	−105.1 (T)	52.5

for these substances are listed in Table XXX. The spin systems of the spectra coincide with the molecular structure in each case (see Section III.B).

3. Solid-State NMR Spectroscopy

The ^{31}P MAS–NMR spectra of the phosphorus oxide sulfides $P_4O_6S_n$ (n = 0–4) have been reported (*80, 162*). $P_4O_6S_2$ and $P_4O_6S_3$ show more isotropic signals than those obtained from solutions of the same compounds (see above). The spectrum of $P_4O_6S_2$ comprises two isotropic signals for P(III) and two for P(V), and the spectrum of $P_4O_6S_3$ shows one signal for P(III) and three signals for P(V). The intensity ratio in both cases is 1:1:1:1. This means that the crystallographically independent (however, within the limits of accuracy of the structure determination, geometrically equivalent) phosphorus atoms produce different signals in the solid-state NMR spectrum. In contrast, the spectrum of P_4O_6S shows only one isotropic signal for P(III) and one for P(V), the intensity ratio being 3:1. This effect is explained by rapid rotational jumps of the molecules around their threefold axis. Low-temperature measurements (at −100°C) show that the P(III) signal splits into three components of approximately equal intensity, as is expected from the crystallographic data. The spectrum of $P_4O_6S_4$ shows only one isotropic signal because of the crystallographical equivalence

of all four phosphorus atoms in the molecule. This signal exhibits a remarkably broad half width and can be interpreted as the superposition of four signals that have approximately equal intensity and have half widths corresponding to those of the signals of the other oxide sulfides (see P_4O_{10} in Section II.C). The differences between the chemical shifts of the isotropic signals of the solid substances and those obtained from solutions are less than 9 ppm. This shows that lattice effects have only marginal impact. Graphical analyses of the side band patterns [corresponding to Herzfeld and Berger (*133*)] yield the principal axes of the shielding tensors and the amounts of the anisotropic chemical shifts. These values are listed in Table XXXI. Within the range of experimental error, with one exception, all tensors of the anisotropic chemical shift show positive axialities. For ^{31}P there exists only one plausible orientation of the tensors with axial symmetry within molecules of the given structure, namely, with its largest component, σ_{II}, along the P=X bond or in the P(III)-lone-pair direction. The shielding tensor of P(III) in P_4O_6S seems to have negative axiality, but this observation can be explained by assuming rotation of the molecule around the threefold axis at room temperature. This interpretation has been confirmed by low-temperature measurements. Figure 22 shows

TABLE XXXI

COMPARISON OF THE OBSERVED AND CALCULATED ^{31}P NMR DATA OF PHOSPHORUS OXIDE SULFIDES $P_4O_6S_n$ (n = 0–4) (*162*)

	P_4O_6	P_4O_6S	$P_4O_6S_2$	$P_4O_6S_3$	$P_4O_6S_4$
P(V)					
σ_{11} (obs)		−125	−136	−145	−137
(calc)		−141	−154	−159	−149
σ_{22} (obs)		−125	−136	−145	−137
(calc)		−141	−145	−151	−149
σ_{33} (obs)		+205	+200	+226	+240
(calc)		+227	+233	+245	+254
σ_{iso} (obs)		−15.3	−23.7	−21.0	−11.1
(calc)		−18.2	−22.1	−21.2	−14.9
P(III)					
σ_{11} (obs)	−230	−95	−218	−176	
(calc)	−202	−209	−209	−171	
σ_{22} (obs)	−230	−95	−218	−176	
(calc)	−202	−201	−189	−171	
σ_{33} (obs)	+120	−178	+90	+103	
(calc)	+139	+133	+131	+138	
σ_{iso} (obs)	−113	−122.6	−115.6	−83.6	
(calc)	−88.2	−92.4	−89.2	−68.2	

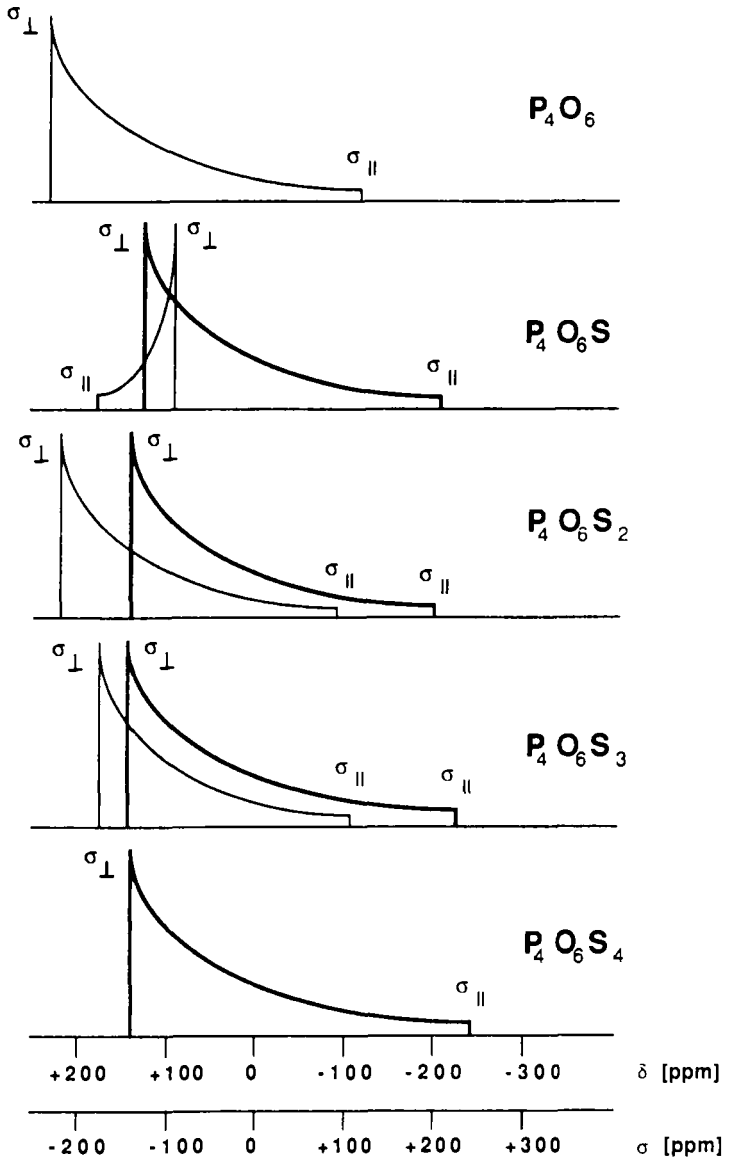

FIG. 22. Schematic representation of the ^{31}P shielding tensors of phosphorus oxide sulfides (*162*).

schematically the shielding tensors for static samples that have been simulated using the experimental MAS data.

For P(V), the value of σ_{II} increases from +205 ppm (P_4O_6S) to +240 ppm ($P_4O_6S_4$), with an increasing number of terminally bonded sulfur

atoms, whereas $\sigma_\perp$ remains approximately constant at −135 ppm. This effect is correlated with the decreasing length of the P=S bond, which implies a higher electron density. In contrast, for the P(III) tensors σ_{II} remains approximately constant at +100 ppm, whereas $\sigma_\perp$ increases from −230 ppm (P_4O_6) to −176 ppm ($P_4O_6S_3$), with an increasing number of terminally bonded sulfur atoms. The matrix elements of the anisotropic shielding tensors as calculated by the individual gauge for localized orbitals (IGLO) method (*130*) are compared with the data obtained experimentally in Table XXXI; except for P_4O_6S, the agreement is convincing.

4. X-Ray Absorption Spectroscopy

The X-ray photoabsorption spectra of the gaseous phosphorus oxide sulfides $P_4O_6S_n$ (n = 1–4) have been recorded for the phosphorus K edge (*80, 186*). The energies of the XANES absorptions are listed in Table XXXII; the spectra are depicted in Fig. 23. The white line in the spectrum of $P_4O_6S_4$ appears at 2150.1 eV. This value is 2.7 eV larger than the corresponding one for P_4O_6, illustrating the dependence of X-ray absorption on the valency of the absorbing atom. In addition, the energy difference between the white lines of P_4O_6 and $P_4O_6S_4$ is much smaller than that between P_4O_6 and P_4O_{10}; this is obviously due to the lower electronegativity of sulfur with respect to oxygen.

Considering the spectra of the phosphorus(III/V) oxide sulfides, it is seen that the absorption at 2148 eV increases in intensity with an increasing number of terminally bonded sulfur atoms, whereas the bands above 2149.5 eV decrease. This effect is explained by the increasing amount of P(III) and the correspondingly decreasing amount of P(V). This phenomenon is further illustrated by simulated spectra that have been obtained by simply adding the spectra of P_4O_6 and $(PhO)_3$-P=S. The striking similarity between the simulated and the observed spectra indicates that the relevant molecular orbitals are highly localized and that it is sufficient to consider the first coordination shells to explain the main features of the XANES absorptions. At room tempera-

TABLE XXXII

P(1s)-XANES ABSORPTIONS (eV) OF PHOSPHORUS OXIDE SULFIDES (*80*)

P_4O_6S	2147.8	2149.7	2150.5 2151.6	2152.9	
$P_4O_6S_2$	2148.4	2150.3	2151.1	2152.2	2153.3
$P_4O_6S_3$	2148.2	2150.1	2150.9	2152.1	2153.4
$P_4O_6S_4$		2150.1		2152.5	2153.6

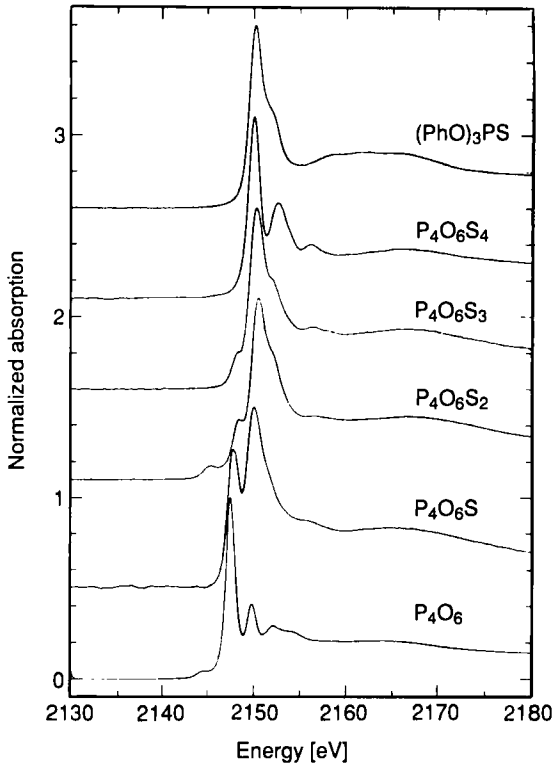

FIG. 23. XANES spectra of phosphorus oxide sulfides (*80, 186*).

ture, the XANES spectrum of P_4O_6S fits well into the trends shown by the other phosphorus oxide sulfides (*134*). Surprisingly, the intensities of the absorption bands change upon heating the sample. Decomposition of the substance could be definitely excluded, because the effect is reversible. This phenomenon is not understood so far.

5. *Photoelectron and Auger Electron Spectroscopy*

The P(1*s*) and P(2*p*) binding energies in P_4O_6S, $P_4O_6S_2$, and $P_4O_6S_4$ have been determined (*80*). As it would be expected, the ionization potentials increase with the increasing oxidation state of the phosphorus atom. Astonishingly, they seem to be independent of the electronegativity of the terminally bonded chalcogen atom; e.g., the P(1*s*) and P(2*p*) binding energies are approximately the same in P_4O_{10} and $P_4O_6S_4$, respectively. This observation can be explained by the fact that both σ attraction and π back-donation of sulfur are less effective than those

in the case of oxygen. As a result, the electron density of phosphorus in $(RO)_3P{=}O$ is approximately the same as that in $(RO)_3P{=}S$.

The XPS and P-KLL Auger electron spectra of the phosphorus(III/V) oxide sulfides P_4O_6S and $P_4O_6S_2$ (*80*) do not show any significant splitting as would be expected due to the different oxidation states of phosphorus. This finding has not been understood so far; further experimental and theoretical work is required.

D. Theoretical Studies

The relative stabilities of the structural isomers $P_4O_6S_4$ (with a P_4O_6 cage) and $P_4S_6O_4$ (with a P_4S_6 cage) have been discussed with reference to the hypothetic adamantane-like O_{14}^{4+} system (*183*). In this "uniform reference frame," the bridge atom sites have negative partial charges with respect to the bridgehead atoms, but the locations of highest negative charge density are the terminal or exoatom sites. By replacing O atoms with P and S atoms, the "rule of topological charge stabilization," which was derived in Ref. (*184*), becomes effective. This rule claims that—in comparison to the reference frame—the heteroatoms are preferentially located in positions where the electron density is accumulated or depleted due to connectivities and electron levels, respectively. Atoms with low electronegativity would prefer positions of low charge density and vice versa. Thus $P_4S_6O_4$ should be more stable than $P_4O_6S_4$. But, as was discussed in Ref. *182*, the experience of synthetic chemistry casts some doubt on this conclusion. Furthermore, the known phosphorus oxide sulfide of the formula $P_4S_6O_4$ has the structure shown in Fig. 21 (*182*), which is in contradiction to the above theoretical results.

The surprising fact that the geometry of the P_4O_6 cage in P_4O_7 and P_4O_6S remains virtually unchanged upon substitution of the terminal oxygen atom through a sulfur atom has been investigated (*165*) by SCF calculations with the TURBOMOLE program. The Mulliken population analyses of P_4O_6S and P_4O_7 show that the most pronounced differences appear at P(V), whereas the charges of all other atoms are much less affected. Furthermore, the charge distributions on *s*, *p*, and *d* orbitals (except for the terminal P—O— or P—S— bond) remain constant. A more detailed analysis (*185*) demonstrated that population analysis might not be reliable because of the high polarity of the molecules.

Moreover, attempts to compare the differences of the electronic energies in P_4O_6S and in P_4O_7, considering either the real or the undistorted geometry of the P_4O_6 cage, have failed because the resulting differences

are far smaller than the variation of the core repulsion energies due to the shortening and lengthening of the P–O_b bonds. This failure suggested the use of P(1*s*) energy as a standard for the effective charges (*165*) (see Section II.D) and thus the correlation of the P(1*s*) energy with the distortion of the cage. As already pointed out in Section II.D, there exists a strong correlation between P(1*s*) energies and distortion of the P_4O_6 cage. Here again the geometrical equivalence is reflected by the P(1*s*) energies, which are approximately the same for P_4O_6S and P_4O_7. It appears as if sulfur terminally bonded to phosphorus has the same "effective electronegativity" as oxygen attached to the same position, in spite of the fact that oxygen has the higher "standard" electronegativity. On the other hand, the electron density of the P=O bond exceeds that of the P=S bond. Thus one could explain the same effective electronegativities of oxygen and sulfur in this situation by assuming that sulfur has a more pronounced ability to accomodate additional electron density.

IV. Comparative Considerations

The synthetic approaches to molecular phosphorus(III/V) oxides and oxide sulfides have some features in common: The compounds P_4O_6X (X = O, S) are prepared from the lowest oxidized member of the $P_4O_6X_n$ series (P_4O_6 itself) by the reactions

$$P_4O_6 \xrightarrow[Ag_2O]{[O_2]} P_4O_7$$

and

$$P_4O_6 \xrightarrow{P_4S_{10}} P_4O_6S,$$

whereas $P_4O_6S_3$ is obtained by the reduction of the highest oxidized members of the $P_4O_6X_n$ series (P_4O_{10} and $P_4O_6S_4$) by the reactions

$$P_4O_{10} \xrightarrow{P_{red} \text{ or } P_{white}} P_4O_9$$

and

$$P_4O_6S_4 \xrightarrow{PPh_3} P_4O_6S_3.$$

However, much more striking are the general differences in reactivity encountered during the syntheses of oxides and oxide sulfides. Due to the higher oxidation capability of oxygen compared with sulfur, the reaction conditions for the preparation of pure P_4O_7 must be fixed much more carefully. As has been pointed out in Sections II.A and III.A, the reaction of P_4O_6 and O_2 takes place at room temperature, whereas the reaction of P_4O_6 with elemental sulfur requires elevated temperatures.

In addition, it is generally much easier to produce $P_4O_6S_n$ in a pure state than to produce the corresponding phosphorus oxides. This fact is mainly due to the tendency of the oxides to form solid solutions, which is favored by the close relationships in metrics and symmetries of their crystal structures. These relationships might be a consequence of the fact that differences in the molecular volumes of the members of the $P_4O_6O_n$ family are smaller than those of the members of the $P_4O_6S_n$ family. Further, synthesis and purification of the oxide sulfides are facilitated by the better solubility of the higher sulfurized members in organic solvents.

Besides the differences in the molecular packings already mentioned in Sections II.B and III.B, the distortions of the P_4O_6 cages vary depending on whether oxygen or sulfur atoms are added. This is as expected and can be attributed to the different abilities of oxygen and sulfur to withdraw electron density from the cage. The only exception to this rule is the couple P_4O_6S and P_4O_7, for which the P_4O_6 cages exhibit approximately the same distortion. As has been discussed in Section III.D, these similarities are a result of two competing effects, which lead to approximately equal "effective" electronegativities of sulfur and oxygen in that special situation.

Variations in the electronic properties of the $P_4O_6X_n$ molecules with respect to the type of the terminally bonded atoms have been investigated using several different spectroscopic techniques. The isotropic ^{31}P NMR shifts of the oxides and the oxide sulfides differ considerably (oxides, -53 to -35 ppm; oxide sulfides, 11 to 25 ppm; reference, H_3PO_4) and are most pronounced for P(V). Using ^{31}P MAS–NMR investigations, it has been demonstrated that these effects mainly are derived from different $\sigma_\perp$ values. Compared with the electron density at the P=S unit, that at the P=O unit seems to be more concentrated along the direction of the bond axis, leading to a higher component in the shielding tensor in this direction. As shown by XPS and especially by XANES spectra, the core binding energies of the phosphorus atoms are significantly affected by the type and number of the terminally bonded atoms. The position of the white line on the energy scale is correlated with the electronegativities of the substituents. Thus the

white line of P_4O_{10} is shifted by 1.7 eV to higher energies compared with that of $P_4O_6S_4$. Even the core electrons of the phosphorus(III) atoms, which are not directly involved in these substitutions, show some sensitivity to the terminally bonded chalcogen atoms. Although the positions of the XANES resonances that are assigned to P(III)-$1s \rightarrow \sigma^*$[P(III)–O] transitions are not affected upon substitution of the terminally bonded oxygen atoms through sulfur atoms, their intensities differ significantly.

V. Concluding Remarks

The preceding sections reveal the substantial gain that has been realized in our knowledge about phosphorus oxides and oxide sulfides. In striking contrast to earlier findings, each individual member of this family of compounds that is notoriously sensitive to moisture has been synthesized, or seems to be accessible, as a pure solid. Most of the compounds have been studied thoroughly with respect to their molecular and crystal structures, giving a sound basis for systematic comparisons. The first attempts to correlate geometric features of the molecules and their electronic structures have been undertaken. However, further experimental input, as well as thorough quantum mechanical descriptions including core states, is needed.

Besides filling in the missing links, it would be desirable to consider in addition the phosphorus oxide selenides. With their inclusion, the tendencies already detected in the oxides and oxide sulfides should become much more pronounced. Furthermore, one would introduce an additional probe atom (^{77}Se) for NMR, a powerful analytical technique in this context.

A preparative chemistry based on phosphorus oxides or oxide sulfides as educts has not been developed. Especially for the binary oxides, a high potential—both in solid state and in molecular chemistry—is obvious in this regard. Knowing that demands to avoid intermediates containing chlorine are arising, even a broad application of phosphorus oxides in technical chemistry becomes imagineable. For this purpose the yields in producing P_4O_6 and especially the phosphorus(III/V) oxides have to be improved considerably, which is a challenge even at the present state of knowledge.

ACKNOWLEDGMENTS

Financial support by the DFG (SFB 334 and Gottfried Wilhelm Leibniz-Programm) and the Fonds der Chemischen Industrie is gratefully acknowledged.

REFERENCES

1. Berzelius, J. J., *Gilbert's Ann.* **53,** 393 (1816).
2. Thorpe, T. E., and Tutton, A. E., *J. Chem. Soc.* **49,** 883 (1886).
3. Thorpe, T. E., and Tutton, A. E., *J. Chem. Soc.* **59,** 1019 (1891).
4. Thorpe, T. E., and Tutton, A. E., *Z. Anorg. Chem.* **1,** 5 (1891).
5. West, C. A., *J. Chem. Soc.* **81,** 923 (1902).
6. Jost, K.-H., *Acta Cryst.* **17,** 1593 (1964).
7. Jost, K.-H., *Acta Cryst.* **21,** 34 (1966).
8. Meisel, M., *Z. Chem.* **23,** 117 (1983).
9. Boyle, R., *Phil. Trans.* **18,** 478 (1694).
10. Davy, H., *Phil. Trans.* **102,** 405 (1821).
11. Dulong, P. L., *Phil. Mag.* **48,** 271 (1816).
12. Berzelius, J. J., *in* "Lehrbuch der Chemie," Vol. II, p. 499 (1825).
13. Delalande, Z., *Ann. Chim. Phys.* **1**(3), 117 (1841).
14. Marchand, R. F., *J. Prakt. Chem.* **16**(1), 373 (1839).
15. Grabovsky, A. G., *Sitzungsber. Akad. Wien* **52,** 170 (1865).
16. Goldschmidt, T,. D.R.P. No. 110,174 (1899).
17. Pistor, G., D.R.P. No. 426,388 (1924).
18. Finch, G. I., Peto, R. H. K., *J. Chem. Soc.* **121,** 692 (1922).
19. Whitaker, H., *J. Chem. Soc.* **127,** 2219 (1925).
20. Threlfall, R., *Phil. Mag.* **35**(5), 1 (1893).
21. Shenstone, W. A., Beck, C. R., *J. Chem. Soc.* **63,** 475 (1893).
22. Kempf, R., *J. Prakt. Chem.* **78**(2), 201 (1908).
23. "Ullmann's Enzyklopädie der Technischen Chemie," Vol. XVIII, p. 303f. Verlag Chemie, Weinheim, 1979.
24. Davy, H., thesis, London, 1800.
25. Dalton, J., *Ann. Phil.* **9,** 186 (1807).
26. Geuther, A., and Michaelis, A., *Chem. Ber.* **4,** 766 (1871).
27. Oddo, G., *Atti Accad. Linc.* **10**(5), 452 (1901).
28. Baumgarten, P., and Brandenburg, C., *Chem. Ber.* **72,** 555 (1939).
29. le Sage, B. G., *Mém. Acad.,* 321 (1777).
30. Lavoisier, A. L., *Mém. Acad.,* 65 (1777).
31. Steinacher, P. A., *Gehlen's J.* **1,** 681 (1803).
32. Reinitzer, B., *Chem. Ber.* **14,** 1884 (1881).
33. Emeléus, H. J., *J. Chem. Soc.* **127,** 1362 (1925).
34. Miller, C. C., *J. Chem. Soc.,* 1847 (1928).
35. Miller, C. C., *J. Chem. Soc.,* 1823 (1929).
36. Heinz, D., *Z. Anorg. Allg. Chem.* **347,** 167 (1966).
37. Walker, M. L., and Mills, J. L., *Syn. Reactivity Inorg. Metal-Org. Chem.* **5,** 29 (1975).
38. Wolf, L., and Schmager, H., *Chem. Ber.* **62,** 771 (1929).
39. Wolf, L., D.R.P. No. 444,664 (1927).
40. Heinz, D., and Thilo, E., East German Patent No. 26,660 (1960).
41. Thilo, E., and Heinz, D., German Patent No. 1,172,241 (1964).
42. Heinz, D., Asijew, R. G., Müller, I. F., and Kauschka, G., *Pure Appl. Chem.* **52,** 825 (1980).
43. Whyte, D. D., Pflaumer, P. F., and Roberts, T. S., French Patent No. 1,531,913 (1968).
44. Heinz, D., Neumann, P., and Crahmer, H., East German Patent No. 1.956,999 (1970).

45. Heinz, D., Crahmer, H., and Neumann, P., German Patent No. 2,028,239 (1971).
46. Krause, H. H., McNulty, J. S., and Hall, R. E., U.S.P. No. 3,652,213 (1972).
47. Mezey, E. J., and Hall, R. E., U.S.P. No. 3,652,211 (1972).
48. Hertzog, K., East German Patent No. 139,426 (1980).
49. Mustroph, G., Kurze, R., Ober, D., Schneider, H., Hofmann, F.-R., Busch, D., Rothe, H., and Kuhnert, E., German Patent No. 288,139 (1991).
50. Hartmann, K., Hebecker, D., Schneider, H., Kurze, R., Busch, D., Mustroph, G., and Otto, J., German Patent No. 292,367 (1991).
51. Otto, J., Schneider, H., Hartmann, K., Hebecker, D., and Kurze, R., German Patent No. 292,636 (1991).
52. Nacquet, A., *in* "Grundzüge der modernen Chemie," p. 218.
53. Gautier, A., *Compt. Rend.* **76,** 49,173 (1873).
54. Besson, A., *Compt. Rend.* **124,** 763 (1897).
55. Besson, A., *Compt. Rend.* **125,** 1032 (1897).
56. Chalk, L. J., and Partington, J. R., *J. Chem. Soc.,* 1930 (1927).
57. Krafft, F., and Neumann, R., *Chem. Ber.* **34,** 565 (1901).
58. Wolf, L., Kalaehne, E., and Schmager, H., *Chem. Ber.* **62,** 1441 (1929).
59. Jorissen, W. P., and Tasman, A., *Rec. Trav. Chim. Pays-Bas* **48,** 324 (1929).
60. Hossenlopp, F., McPartlin, M., and Ebel, P. J., *Bull. Soc. Chim,* 791 (1960).
61. v. Druten, A., *Rec. Trav. Chim. Pays-Bas* **48,** 312 (1929).
62. Béchamp, A., *Compt. Rend.* **40,** 944 (1855).
63. Anderson, H. H., *J. Org. Chem.* **19,** 1766 (1954).
64. Jander, G., Wendt, H., and Hecht, H., *Chem. Ber.* **77,** 698 (1944).
65. Hautefeuille, P., and Perrey, A., *Compt. Rend.* **99,** 33 (1884).
66. Russell, E. J., *J. Chem. Soc.* **83,** 1263 (1903).
67. Miller, C. C., *Proc. R. Soc. Edinburgh* **46,** 239 (1926).
68. Britzke, E., and Pestow, N., *Tr. Nauchn. Inst. Udobr.* **59,** 5 (1929).
69. Emmett, P. H., and Schultz, J. F., *Ind. Engr. Chem.* **31,** 105 (1939).
70. Brunauer, S., and Schultz, J. F., *Ind. Engr. Chem.* **33,** 828 (1941).
71. Thilo, E., Heinz, D., and Jost, K.-H., *Angew. Chem.* **76,** 229 (1964).
72. Heinz, D., *Z. Anorg. Allg. Chem.* **336,** 137 (1965).
73. Heinz, D., Rienitz, H., and Radeck, D., *Z. Anorg. Allg. Chem.* **383,** 120 (1971).
74. Ewert, G., Förster, I., Heinz, D., Kauschka, G., and Kurze, R., German Patent No. 294,465 (1991).
75. Loeper, M., and Schülke, U., *Z. Anorg. Allg. Chem.* **500,** 40 (1983).
76. Walker, M. L., and Mills, J. L., *Inorg. Chem.* **16,** 3033 (1977).
77. Walker, M. L., Peckenpaugh, D. E., and Mills, J. L., *Inorg. Chem.* **18,** 2792 (1979).
78. Jansen, M., and Voss, M., *Angew. Chem.* **93,** 120 (1981).
79. Jansen, M., and Moebs, M., *Z. Anorg. Allg. Chem.* **514,** 39 (1984).
80. Frick, F., thesis, Bonn, 1993.
81. Jansen, M., and Moebs, M., unpublished results.
82. Lüer, B., thesis, Bonn, 1991.
83. Jansen, M., and Lüer, B., *Z. Krist.* **197,** 247 (1991).
84. Harnisch, H., *Z. Anorg. Allg. Chem.* **300,** 261 (1959).
85. Clade, J., and Jansen, M., unpublished results.
86. Thorpe, T. E., and Tutton, A. E., *J. Chem. Soc.* **57,** 545 (1890).
87. Tilden, A., and Barnett, R. E., *J. Chem. Soc.* **69,** 154 (1896).
88. le Bas, G., *Chem. News* **111,** 113 (1915).
89. Maxwell, L. R., Hendricks, S. B., and Deming, L. S., *J. Chem. Phys.* **5,** 626 (1937).
90. Hampson, G. C., and Stosick, A. J., *J. Am. Chem. Soc.* **60,** 1814 (1938).

91. Beagley, B., Cruickshank, D. W. J., Hewitt, T. G., and Jost, K.-H., *Trans. Faraday. Soc.* **65,** 1219 (1969).
92. Akishin, P. A., Rambidin, N. G., and Zasorin, E. Z., *Kristallografiya* **4,** 360 (1959); *Sov. Phys. Cryst.* **4,** 334 (1959).
93. Beagley, B., Cruickshank, D. W. J., Hewitt, T. G., and Haaland, A., *Trans. Faraday Soc.* **63,** 836 (1967).
94. Thilo, E., and Wieker, W., *Z. Anorg. Allg. Chem.* **277,** 29 (1954).
95. de Decker, H. C. J., and McGillavry, C. H., *Rec. Trav. Chim. Pays-Bas* **60,** 153 (1941).
96. de Decker, H. C. J., *Rec. Trav. Chim. Pays-Bas* **60,** 413 (1941).
97. McGillavry, C. H., de Decker, H. C. J., and Nijland, L. M., *Nature* **164,** 448 (1949).
98. Cruickshank, C. D. J., *Acta Cryst.* **17,** 677 (1964).
99. Jansen, M., and Lüer, B., *Z. Krist.* **177,** 149 (1986).
100. Jansen, M., Voss, M., and Deiseroth, H.-J., *Angew. Chem.* **93,** 1023 (1981).
101. Jansen, M., and Moebs, M., *Inorg. Chem.* **23,** 4486 (1984).
102. Jansen, M., and Wipperfürth, P., unpublished results.
103. Jost, K.-H., and Schneider, M., *Acta Crystrallogr. B* **37,** 222 (1981).
104. Gillespie, R. J., *in* "Molekülgeometrie, Elektronenpaar-Abstoßung und molekulare Struktur." Verlag Chemie, Weinheim, 1975.
105. Jansen, M., and Moebs, M., *Z. Krist.* **159,** 283 (1982).
106. Kitaigorodski, A. I., *in* "Molekülkristalle." Akademie Verlag, Berlin, 1979.
107. Gerding, H., v. Brederode, H., and de Decker, H. C. J., *Rec. Trav. Chim. Pays-Bas* **62,** 549 (1942).
108. Gerding, H., and de Decker, H. C. J., *Rec. Trav. Chim. Pays-Bas* **64,** 191 (1945).
109. v. Brederode, H., and Gerding, H., *Rec. Trav. Chim. Pays-Bas* **67,** 677 (1948).
110. Gerding, H., *J. Chim. Phys.* **46,** 118 (1948).
111. Sidorov, T. A., and Sobolev, N. N., *Opt. Spektr.* **2,** 710,717 (1957).
112. Sidorov, T. A., and Sobolev, N. N., *Fiz. Sborn.* **3,** 148 (1957).
113. Zijp, D. H., *Adv. Mol. Spectrosc.* **1–3,** 345 (1962).
114. Chapman, A. C., *Spectrochim. Acta A* **24,** 1687 (1968).
115. Beattie, I. R., Livingston, K. M. S., Ozin, G. A., and Reynolds, D. J., *J. Chem. Soc. A,* 449 (1970).
116. Konings, R. J. M., Cordfunke, E. H. P., and Booij, A. S., *J. Mol. Spectroscopy* **152,** 29 (1992).
117. Mielke, Z., and Andrews, L., *J. Phys. Chem.* **93,** 2971 (1989).
118. Mielke, Z., and Andrews, L., *Inorg. Chem.* **29,** 2773 (1990).
119. McCluskey, M., and Andrews, L., *J. Phys. Chem.* **95,** 3545 (1991).
120. Muldagaliev, Kh. Kh., Mirgorodskii, A. P., and Lazarev, A. N., *Neorg. Mater.* **8,** 81 (1972).
121. Jansen, M., Clade, J., and Frick, F., unpublished results.
122. Chapman, A. C., Homer, J., Mowthorpe, D. J., and Jones, R. T,. *Chem. Commun.,* 121 (1965).
123. Cruickshank, D. W. J., *J. Chem. Soc.,* 5486 (1961).
124. Goubeau, J., *Pure Appl. Chem.* **44,** 393 (1975).
125. Walker, M. L., and Mills, J. L., *Inorg. Chem.* **14,** 2438 (1975).
126. Grimmer, A.-R., and Wolf, G.-U., *Eur. J. Solid State Inorg. Chem.* **28,** 221 (1991).
127. Grimmer, A.-R., and Müller, D., *Z. Chem.* **16,** 496 (1976).
128. Grimmer, A.-R., *Z. Chem.* **18,** 233 (1978).
129. Grimmer, A.-R., *Resonance Relat. Phen.* **20,** 483 (1979).
130. Schindler, M., and Kutzelnigg, W., *J. Chem. Phys.* **76,** 1919 (1982).
131. Mowthorpe, D. J., and Chapman, A. C., *Mol. Phys.* **15,** 429 (1968).

132. Aksnes, D. W., *Acta Chem. Scand.* **23,** 1078 (1969).
133. Herzfeld, J., and Berger, A., *J. Chem. Phys.* **73,** 6021 (1980).
134. Redeker, A., Küper, G., Hormes, J., Frick, F., Jansen, M., and Mühlhäuser, M., *Phosphorus, Sulfur Silicon* **76,** 239 (1993).
135. Küper, G., Chauvistré, R., Hormes, J., Frick, F., Jansen, M. Lüer, B., and Hartmann, E., *Chem. Phys.* **165,** 405 (1992).
136. Sodhi, R. N., and Cavell, R. G., *J. Electron Spectrosc. Relat. Phen.* **32,** 283 (1983).
137. Dake, C. S., Baer, D. R., and Friedrich, D. M., *J. Vacuum Sci. Technol. A* **7,** 1634 (1989).
138. Franke, R., Chassé, T., Al-Araj, B., Streubel, P., and Meisel, A., *Phys. Stat. Solid. B* **160,** 143 (1990).
139. Franke, V., Chassé, T., Streubel, P., and Meisel, A., *J. Electron Spectrosc. Relat. Phen.* **56,** 381 (1991).
140. Hormes, J., and Redeker, A., unpublished results.
141. Egdell, R. G., Palmer M. L., and Findlay, R. H., *Inorg. Chem.* **19,** 1314 (1980).
142. Brundle, C. R., Kuebler, N. A., Robin, M. B., and Basch, H., *Inorg. Chem.* **11,** 20 (1972).
143. Evans, S., Joachim, P. J., Orchard, A. F., and Turner, D. W., *Int. J. Mass Spectrosc. Ion Phys.* **9,** 41 (1972).
144. Tahri, Y., and Chermette, H., *J. Electron Spectrosc.* **56,** 51 (1991).
145. Makarov, L. L., Zaitsev, Yu. M., and Batrakov, Yu. F., *Theor. Eksperim Khim.* **12,** 78 (1976).
146. Makarov, L. L., Zaitsev, Yu. M., and Batrakov, Yu. F., *Izv. Akad. Nauk SSSR, Ser. Fiz.* **40,** 399 (1976).
147. Fluck, E., and Weber, D., *Z. Naturf. B* **29,** 603 (1974).
148. Lee, T. H., Jolly, W. L., Bakke, A. A., Weiss, R., and Verkade, J. G., *J. Am. Chem. Soc.* **102,** 2633 (1980).
149. Rose, J. L., VanCott, T. C., Schatz, P. N., Boyle, M. E., and Palmer, M. H., *J. Phys. Chem.* **93,** 3504 (1989).
150. Bak, B., Kristiansen, N. A., and Svanholt, H., *J. Mol. Struct.* **78,** 63 (1982).
151. Hashizume, A., Wasada, N., and Tsuchiya, T., *Bull. Soc. Chem. Jpn.* **39,** 150 (1966).
152. Daasch, L. W., Weber, J. N., Ebner, M. A., and Sparrow, G., *J. Mass Spectrosc. Ion Phys.* **2,** 503 (1969).
153. Muenow, D. W., Uy, O. M., and Margrave, J. L., *J. Inorg. Nucl. Chem.* **32,** 3459 (1970).
154. Southard, J. C., and Nelson, R. A., *J. Am. Chem. Soc.* **59,** 911 (1937).
155. Hill, W. L., Faust, G. T., and Hendricks, S. B., *J. Am. Chem. Soc.* **65,** 794 (1943).
156. Smits, A., *Z. Phys. Chem. B.* **46,** 43 (1940).
157. Smits, A.; and Rutgers, A. J., *J. Chem. Soc.* **125,** 2573 (1924).
158. Frandsen, M., *Bur. Standard J. Res.* **10,** 54 (1933).
159. Hoeflake, J. M. A., and Scheffer, F. E. C., *Rec. Trav. Chim. Pays-Bas* **45,** 191 (1926).
160. Hartley, S. B., and McCoubry, J. C., *Nature* **198,** 476 (1963).
161. Koerner, W. B., and Daniels, E., *J. Chem. Phys.* **20,** 113 (1952).
162. Frick, F., Hoffbauer, W., Grimmer, A. R., Jansen, M., Fleischer, U., and Kutzelnigg, W., *Naturwiss.* **80,** 465 (1993).
163. McAloon, B. J., and Perkins, P. G., *Theor. Chim. Acta* **24,** 102 (1972).
164. Kutzelnigg, W., *Angew. Chem.* **96,** 262 (1984).
165. Mühlhäuser, M., Engels, B., Marian, C. M., Peyerimhoff, S. D., Bruna, P. J., and Jansen, M., *Angew. Chem.*, **106,** 578 (1994).

166. Frick, F., Jansen, M., Bruna, P. J., and Peyerimhoff, S. D., *Chem. Ber.* **124,** 1711 (1991).
167. Besson, A., *Compt. Rend.* **124,** 151 (1897).
168. Abel, E. W., Armitage, D. A., and Bush, R. P., *J. Chem. Soc. Suppl.* **1,** 5584 (1964).
169. Baeker, M., Heinz, D., Kurze, R., and Radeck, D., East German patent No. 101,368 (1973).
170. Walker, M. L., thesis, Texas Technical University, 1976.
171. Pernert, J. C., and Brown, I. H., U.S.P. No. 2,577,207 (1951).
172. Pernert, J. C., *Chem. Eng. News* **27,** 2143 (1949).
173. Wolf, G.-U., and Meisel, M., *Z. Anorg. Allg. Chem.* **509,** 101 (1984).
174. Stock, A., and Friederici, K., *Chem. Ber.* **46,** 1380 (1913).
175. Frick, F., and Jansen, M., *Z. Anorg. Allg. Chem.* **619,** 281 (1993).
176. Stosick, A. J., *J. Am. Chem. Soc.* **61,** 1130 (1939).
177. Mijlhoff, F. C., Portheine, J., and Romers, C., *Rec. Trav. Chim. Pays-Bas* **86,** 257 (1967).
178. Wolf, G.-U., and Meisel, M., *Z. Chem.* **20,** 451 (1980).
179. Palkina, K. K., Maksimova, S. I., and Wolf, G.-U., *Neorg. Mat.* **16,** 1466 (1980).
180. Gerding, H., and v. Brederode, H., *Rec. Trav. Chim. Pays-Bas* **64,** 183 (1945).
181. van Wazer, J. R., Callis, C. F., Shoolery, J. N., and Jones, R. C., *J. Am. Chem. Soc.* **78,** 5715 (1956).
182. Grunze, H., *Pure Appl. Chem.* **52,** 799 (1980).
183. B. M. Gimarc, and J. J. Ott, *J. Am. Chem. Soc.* **108,** 4298 (1986).
184. Gimarc, B. M., *J. Am. Chem. Soc.* **105,** 1979 (1983).
185. Engels, B., Mühlhäuser, M., Peyerimhoff, S. D., and Jansen, M., unpublished results.
186. Pantelouris, A., Hormes, J. Günther, C., Hartmann, E., Frick, F., and Jansen, M., *Chem. Phys.,* in press.